This manuscript is a preprint and has been submitted for publication in Phil. Trans. Roy. Soc. It has not yet undergone any peer review.

Submitted to Phil. Trans. R. Soc. A - Issue

This manuscript has not yet undergone peer review

PHILOSOPHICAL TRANSACTIONS
OF THE ROYAL SOCIETY A
MATHEMATICAL, PHYSICAL AND ENGINEERING SCIENCES

What's down there? The structures, materials and environment of deep-seated tremor and slip

Journal:	*Philosophical Transactions A*
Manuscript ID	Draft
Article Type:	Review
Date Submitted by the Author:	n/a
Complete List of Authors:	Behr, Whitney; Eidgenössische Technische Hochschule Zürich, Department of Earth Sciences Burgmann, Roland; University of California Berkeley, Earth and Planetary Science
Issue Code (this should have already been entered and appear below the blue box, but please contact the Editorial Office if it is not present):	DM02202
Subject:	Geophysics < EARTH SCIENCES, Plate tectonics < EARTH SCIENCES, Geology < EARTH SCIENCES
Keywords:	episodic tremor and slip (ETS), subduction plate interface, tremor and slow slip events, subduction megathrust earthquakes, subduction shear zone rheology, melange belts

SCHOLARONE™
Manuscripts

This manuscript has not yet undergone peer review

Author-supplied statements

Relevant information will appear here if provided.

Ethics

Does your article include research that required ethical approval or permits?:
This article does not present research with ethical considerations

Statement (if applicable):
CUST_IF_YES_ETHICS :No data available.

Data

It is a condition of publication that data, code and materials supporting your paper are made publicly available. Does your paper present new data?:
My paper has no data

Statement (if applicable):
CUST_IF_YES_DATA :No data available.

Conflict of interest

I/We declare we have no competing interests

Statement (if applicable):
CUST_STATE_CONFLICT :No data available.

Authors' contributions

This paper has multiple authors and our individual contributions were as below

Statement (if applicable):
Both authors contributed equally to the manuscript writing and assembly.

For Review Only

PROCEEDINGS A

rspa.royalsocietypublishing.org

Research

Article submitted to journal

Subject Areas:

...

Keywords:

...

Author for correspondence:

...

What's down there? The structures, materials and environment of deep-seated tremor and slip

Whitney M. Behr[1], Roland Bürgmann[2]

[1]Geological Institute, Department of Earth Sciences, ETH Zurich (Swiss Federal Institute of Technology), Zurich, Switzerland

[2]Department of Earth and Planetary Science and Berkeley Seismological Laboratory, University of California, Berkeley, CA, USA.

Episodic tremor and slow slip (ETS) events occur downdip of the seismogenic zone of numerous subduction megathrusts and plate boundary strike-slip faults. These events represent a fascinating and perplexing mode of fault failure that has greatly broadened our view of earthquake dynamics. In this contribution, we review constraints on the ETS deformation process from both geophysical observations of active subduction zones and geological observations of exhumed field analogs. We first provide an overview of what has been learned about the environment, kinematics and dynamics of ETS from geodetic and seismologic data. We then describe the materials, deformation mechanisms, and metamorphic and fluid pressure conditions that characterize exhumed rocks from ETS source depths. Both the geophysical and geological records strongly suggest the importance of a fluid-rich and high fluid pressure habitat for the ETS source region. Additionally, transient deformation features preserved in the rock record, involving combined frictional-viscous shear in regions of mixed lithology and near-lithostatic fluid pressures, may scale with the tremor component of ETS events. While several open questions remain, it is clear that improved constraints on the materials, environment, structure, and conditions of the plate interface from geophysical imaging and geologic observations will enhance model representations of the boundary conditions and geometry of the ETS system.

For Review

THE ROYAL SOCIETY PUBLISHING

© The Author(s) Published by the Royal Society. All rights reserved.

This manuscript has not yet undergone peer review

1. Introduction

What was long considered to be bothersome seismic noise and long-period errors in geodetic time series, turned out to be one of the exciting discoveries in the Earth sciences in recent decades; episodic slow slip events (SSE) and associated tremor signals originating deep on the plate interface of the Nankai, Japan, and Cascadia, USA, subduction zones (Figure 1) [1–3]. Ever since their original discovery, we have been wondering what things look like down there; that is, what are the geologic materials and structures of episodic tremor and slip (ETS)?

The "ETS zone" (Figure 2) is located within depth and temperature ranges of about 25-50 km and 400-550°C, which are conditions commonly associated with hot and young subducting oceanic plates, down dip of the "seismogenic zone" hosting regular earthquakes of up to M > 9 [4]. Tremors at similar pressure and temperature conditions are also found in continental plate boundary faults, including the strike-slip San Andreas Fault in California [5], the oblique right-lateral Alpine Fault in New Zealand [6], and the continental collision zone in Taiwan [7] (Figure 1). Down dip of this zone, the plate boundary deformation appears to be steady, accommodated by ductile shear. Up dip of the ETS zone, some subduction zones abut locked sections of the seismogenic megathrust (e.g., Kii Peninsula, Japan), some host larger, longer-lasting and less frequent SSEs (e.g., Tokai and south Shikoku in Japan, Guerrero in Mexico), while others feature a wide, steadily creeping zone with little if any tremor, forming an apparent gap between the ETS zone and locked asperities (Cascadia). In some subduction zones, tremors and slow slip are also found at intermediate and shallow depths [8,9], suggesting that conditions for ETS can exist at all depth ranges of subduction thrusts. Here we focus on the deep-seated ETS zone of subduction zones and their potential analogs exhumed from blueschist to eclogite facies environments.

There is abundant evidence that indicates a close temporal and spatial association of tremor and slow slip [10,11]. Tremors represent enduring low-frequency seismic signals generally interpreted as being a direct byproduct of otherwise slow and aseismic slip. While on average the seismic moment released by tremor amounts to only ~0.1% of the associated slow slip [12,13], tremor is generally considered as a direct marker of the spatio-temporal evolution of slow slip

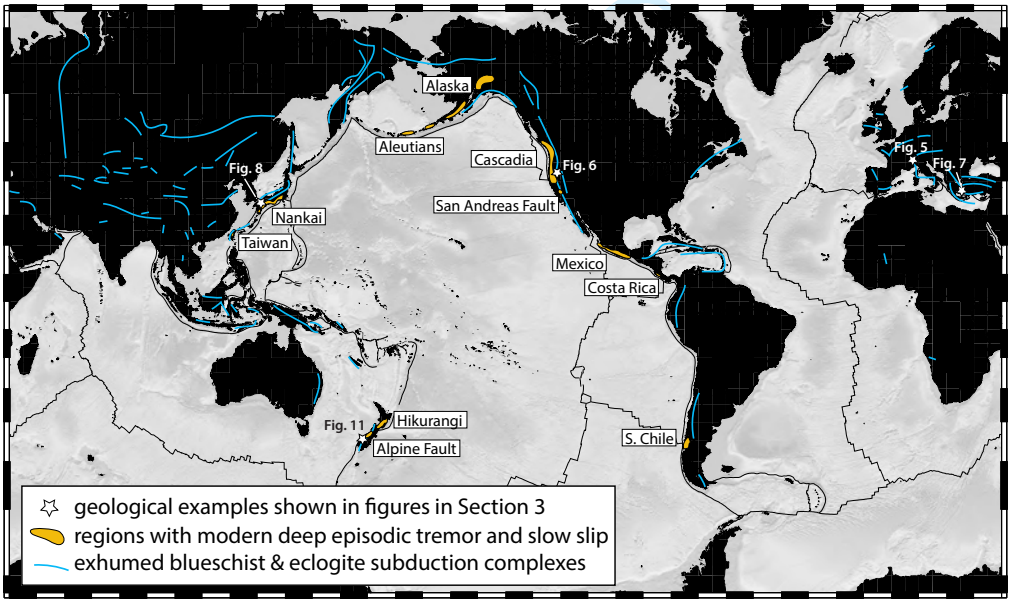

Figure 1. Global distribution of regions with modern deep episodic tremor and slow slip along with exhumed blueschist and eclogite facies subduction complexes.

during an SSE. However, while tremor and slow slip are closely associated, they are not always exactly coincident in space and time. Slow slip may occur without tremor, and smaller SSEs may be indicated by tremor transients, but lack a resolvable geodetic signal [14,15]. The study of small (M « 2.5) low-frequency earthquakes (LFEs) and M 3-4 very low-frequency earthquakes embedded in the tectonic tremor signal allows for more detailed investigation of underlying source properties and the spatio-temporal distribution of fault slip. Thus, accurate locations and source properties of tremors and LFEs are essential ingredients for improved understanding of the slow slip process.

So, what are the rocks and structures preserved in the geologic record that could represent deep tremor and slow slip? An essential aspect of understanding the ETS process is the examination of rocks exhumed from ETS source depths, which are exposed in subduction complexes in a wide range of tectonic settings around the globe (Figure 1). Exhumed subduction complexes can contain slivers of the downgoing slab, the upper plate, and the interface shear zone itself. Through carefully probing these exposures to distinguish subduction versus exhumation features, we can identify "snapshots" of the ETS source region captured at a range of depth and temperature conditions, and use them to provide key insights into lithological and rheological contrasts, short- and long-timescale deformation processes, interplay between deformation and metamorphism, and fluid migration patterns. Observations focused on this topic thus far suggest that rocks preserve a record of both long-term strain accumulated over millions of years, as well as punctuated transient deformation set up in regions where lithologies are mixed, fluids are

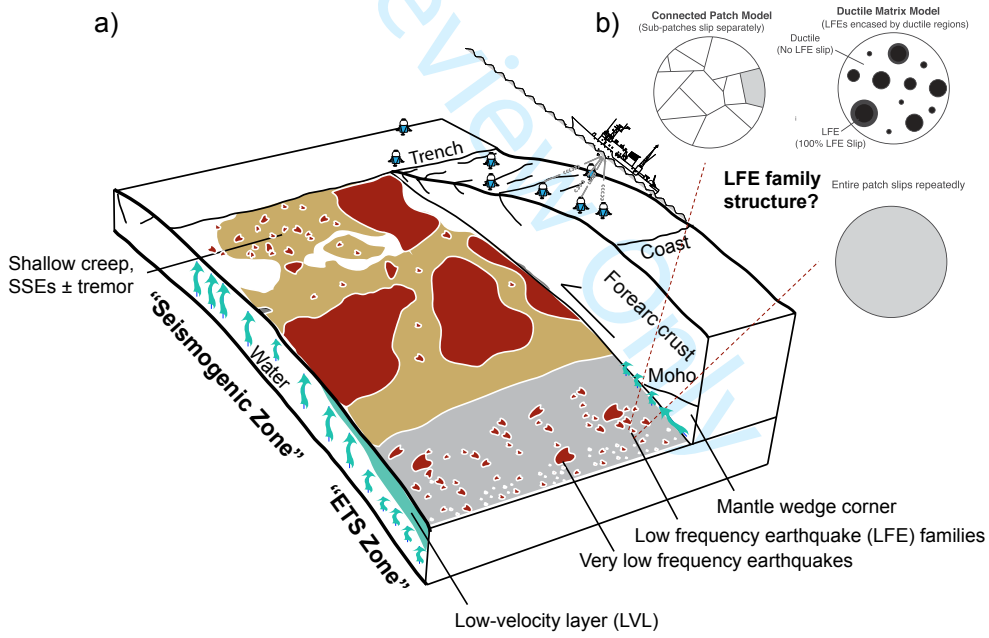

Figure 2. Summary schematic of the geophysical view of episodic tremor and slip (ETS) and informed by geophysical imaging, source seismology and geodesy. Earthquake ruptures in the seismogenic zone, and low frequency earthquakes (LFE) and very low frequency earthquakes in the ETS zone release seismic energy (red patches). The plate interface away from the seismic patches slip by aseismic creep, often in episodic slow slip events. Slow slip in the ETS zone (grey) is illuminated by tremors. LFE source patches are clustered in families that are sometimes aligned in the plate convergence direction. Fluid pressure is likely high along much of the plate interface and reaches lithostatic levels in the ETS zone under the mantle wedge corner and forearc crust. Modified from [4] and [16]. Bursts of events in LFE families may reflect repeated failure of the same patch, connected sub-patches or more distributed source patches in a ductile matrix (schematic in top right based on [13]).

For Review Only

This manuscript has not yet undergone peer review

abundant, and fluid pressures are near-lithostatic. Here we first provide an overview of inferences made from geophysical observations about the environment and deformation processes in the ETS zone and then we review knowledge gained from geological studies of relevant analog field examples. Improved models and understanding of deep slow slip processes in plate boundary faults will require drawing on both types of observations.

2. Geophysical Observations of ETS Environment and Source

Deep-seated ETS represent only a small part of the wide spectrum of seismic and aseismic slip processes that we now recognize to occur across the whole width of the subduction plate interface [16–18]. In this section, we review what has been learned about the environment, the kinematics and the dynamics of ETS from geophysical imaging and geodetic and seismologic observations. We focus on aspects that can potentially be related to findings obtained from geologic analogs of the deep ETS source region.

(a) The Environment of deep ETS

In subduction zones, deep ETS are found near the mantle wedge corner, where the subducting oceanic crust interfaces with the overriding forearc crust and, often serpentinized, continental mantle (Figure 2). The section of the subduction thrust hosting ETS lies near the top or within a zone of low seismic velocities and very high ratios of the *P*-wave and *S*-wave velocities (*Vp/Vs*), the low-velocity layer (LVL) [19–22]. For example, in central Japan, Kato et al. [23] find an LVL with low seismic velocities and high *Vp/Vs* ratios, both along the zone of tremor and long-term SSEs without tremor (Figure 3). Here, a zone of frequent ETS events appears on the deeper plate interface beneath the partially serpentinized mantle wedge, while more enduring years-long SSEs without tremor occur farther up dip, below the forearc crust. In the Cascadia, southwest Japan, Costa Rica, New Zealand, and Alaska subduction zones, the maximum *Vp/Vs* regions and ETS zones also appear to roughly coincide with the intersection of the subducting plate with the mantle wedge corner [24].

There continues to be some debate about the makeup and state of the LVL. Based on seismic data from northern Cascadia, Hansen et al. [38] argue that the 3-4 km thickness of the LVL, its high *Vp/Vs* ratio and its limited down-dip extent support the inference of the ETS zone consisting primarily of uppermost oceanic crustal rocks at very high fluid pressures. In contrast, Abers et al. [39] and Calvert et al. [40] favor the LVL being dominated by underplated metasediments. The subduction interface may be fluid saturated and frictionally weak across much of its down-dip width thanks to fluids released by the downgoing slab; however, Audet et al. [33] use onshore-offshore receiver function data to show that the LVL thins offshore and does not extend to the locked section of the megathrust. High electric conductivity is also found in the ETS zone of the Cascadia subduction zone, but not in the locked updip section of the megathrust [41]. Delph et al. [34] find zones with a much thicker (∼10 km) LVL in both the northern and southern Cascadia subduction zone, which appear to correlate with increased tremor rates and seismicity in the underlying slab. This may suggest that thick underplated sediments invaded by slab-derived fluids are related to increased tremor occurrence in those zones [34]. However, from a geophysical perspective alone, the exact makeup of the LVL remains uncertain [33].

Seismic receiver function studies find an anisotropic fabric in the LVL plunging at an oblique angle to the plate interface both in Cascadia and Mexico, suggesting distributed shear and the development of high strain fabrics [22,38]. This supports the idea that the LVL reflects the development of an increasingly thick, fluid-rich and overpressured shear zone hosting both aseismic and ultimately tremor-producing slow slip. LFEs appear to locate within the LVL [33], but the exact vertical distribution of the tremor sources and deformation in the LVL is not well established.

High *Vp/Vs* ratios of 2-3.5, and equivalently Poisson's ratios of 0.33 - 0.46 (Table 1), are consistent with strongly elevated pore fluid pressures in porous (up to 4% porosity) and highly

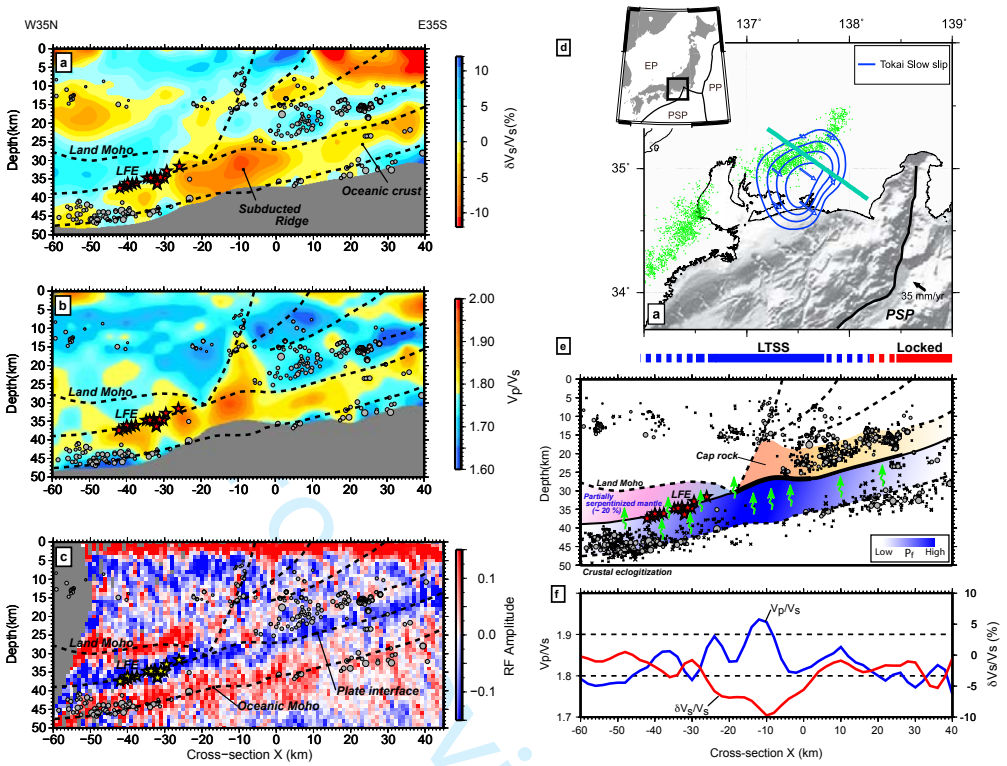

Figure 3. Seismic imaging of Philippine Sea Plate subduction thrust hosting slow slip and tremor beneath Tokai District in central Japan. (a) Depth section of S-wave velocity perturbation (dVs/Vs) from seismic tomography. (b) Ratio of P and S-wave velocities (*Vp/Vs*). (c) Receiver function results (RF amplitude) highlighting sharp changes in seismic velocities that illuminate the plate interface and the continental and oceanic Moho. (d) Map showing slip contours of long-term SSE (blue), low frequency earthquakes (green circles), and northwest-southeast profile line (cyan). (e) Schematic interpretation of seismic structures. Blue shades in subducting oceanic crust reflect fluid pressure variations. Green arrows denote potential fluid pathways in the subduction zone. (f) Profile showing variations of dVs/Vs and *Vp/Vs* within the subducting oceanic crust. Relocated hypocenters are plotted for events within 10 km of the cross-section with gray circles indicating regular earthquakes and red stars indicating LFEs. The deep ETS zone hosts LFEs and M6 slow slip events recurring every few months [25]. An intermediate-depth section of the plate boundary hosts long-term M7 slow slip events (LTSS) that last for years and shorten the deeper ETS recurrences. The updip locked zone fails in M8 megathrust ruptures every ∼150 years. (Images provided by A. Kato based on [23]).

strained metabasalts and metasediments of the subducting oceanic crust [28,42]. The observed velocity ratios suggest pore fluids under near lithostatic pressure, but *Vp/Vs* is also increased in rocks with high fracture densities [43]. The fluids are made available by prograde metamorphic dehydration reactions in the subducting oceanic crust [44]. At these temperatures and pressures, water is a supercritical fluid and is a factor of ∼ten less viscous than near-surface water. Sustaining near lithostatic fluid pressures requires a capping seal with very low vertical permeability [21,28]. This seal may be formed in part by the strongly sheared fault-zone rocks of the plate interface whose permeability is likely strongly anisotropic [36]. Nakajima et al. [45] and Wells et al. [46] relate the distribution of tremor to the degree of metamorphism and distribution of fault zones in the hanging wall of the megathrust, respectively, which appear to provide some control on lower-crustal permeability and thus on the fluid pressure in the LVL.

Audet and Bürgmann [47] find that *Vp/Vs* ratios in the lower crust above the tremor zone are substantially reduced from typical forearc values, consistent with the addition of quartz

This manuscript has not yet undergone peer review

Table 1. Summary list of relevant deep ETS-zone properties from geophysical and laboratory constraints.

Parameter	Constraint or Observable	Typical Values and Notes	References
Depth	Tremor locations and SSE modeling	25 – 50 km (to >60 km in a few areas) [26,27]	[24]
Lithostatic overburden	From depths (Assuming average density 2700 kg m^{-3})	650 – 1200 MPa	
Temperature	From thermomechanical modeling	400-550°C	[28,29]
Major hydrous mineral breakdown reactions	Thermal & petrological modeling	Ultramafic rocks: antigorite, chlorite Mafic rocks: lawsonite, chlorite, glaucophane Metasediments: phengite, lawsonite, chlorite	[30–32]
Geometry of low-velocity layer (LVL) hosting ETS	Seismic tomography and receiver function analysis	~4 ± 1 km-thick (between higher-velocity layers, thinning up-dip and disappearing at ~50 km depth. Can be >>5 km in places.)	[23,24,33,34]
Fluid pressure, effective normal stress	From *Vp/Vs* = 2-3.5 found in receiver function studies (lower-resolution tomography finds somewhat lower values)	~lithostatic (effective normal stress ~1 MPa or less)	[20,24]
Porosity	From *Vp/Vs*, electrical conductivity	3.3-4 %	[28]
Poisson's ratio	From *Vp/Vs* $\sigma = \frac{1}{2}\frac{(Vp^2 - 2Vs^2)}{(Vp^2 - Vs^2)}$	0.33-0.46	
Fluid viscosity	Laboratory	~10^{-4} Pa s	[28]
Permeability	*Vp/Vs* contrast across plate interface and laboratory measurements	<10^{21} m^2 (permeability is likely highly anisotropic and time dependent through the ETS cycle)	[21,35–37]

precipitates (5-15% by volume) to the lower crust [48,49]. In addition, there appears to be a correlation between ETS recurrence intervals and upper-plate silica enrichment, suggesting that increasing quartz-vein mineralization from slab-derived fluids reflects more rapid development of fluid overpressure and therefore shorter recurrence times. This correlation appears to hold both for a number of different subduction zones and for the observed systematic decrease in the recurrence time of ETS with increasing depth of the plate interface in the northern Cascadia subduction zone [47]. These results suggest cycles of slow slip episodes, dilatancy and healing that produce rapid changes in permeability and fluid pressure.

To achieve high fluid pressure, pathways for fluid transport along the megathrust or into the overlying mantle wedge or fore-arc crust may be intermittent [47]. There is some observational evidence, from temporal changes in gravity, seismic velocity, seismic attenuation, seismicity, and state of stress, that indicates pressure changes and fluid transport along and across the fault zone associated with slow slip episodes. In the Tokai District in central Japan (Figure 3), Tanaka et al. [50,51] find absolute gravity changes during two ~5-year-long slow-slip episodes, invoking cycles of fluid pressure and fault zone permeabilities of 10^{18}–10^{15} m^2. In the northern Cascadia subduction zone, Gosselin et al. [52] document seismic velocity changes that may reflect seal breaching and fluid flow in permeable pathways within and away from the megathrust, resulting in transient fluid pressure drops of 1-10 MPa. Nakajima et al. [53] explore temporal changes in slip rate, seismicity and seismic attenuation along the ~50 km deep megathrust of the Philippine Sea in central Japan to infer cyclic drainage episodes from the megathrust. Attenuation and

For Review Only

seismicity in the overriding plate are enhanced within a few months following an SSE, suggesting permeable pathways into the upper plate from near the up-dip edge of the slow slip zone [53]. In the relatively shallow ETS zone of the Hikurangi subduction zone in New Zealand, Warren-Smith et al. [54] document time-dependent variations in the state of stress in the underlying, overpressured oceanic crust from focal mechanism data. The data are interpreted as being the result of inter-SSE rise and co-SSE drop of fluid pressure in the overpressured zone by several MPa, reflecting multiple cycles governed by fracture and healing processes in the plate boundary zone [54] .

(b) ETS and Tremor Source Characteristics

Inversions of geodetic time series (from GPS, tilt- and strainmeters) and the spatio-temporal distribution of tremors paint a picture of highly dynamic slow slip processes on the deep plate interface below the seismogenic zone (Figure 4). These slow slip transients span a wide range of many orders of magnitude in dimension, rate and duration (see Table 2 for typical values and related references). Here we summarize the slow slip behavior in the ETS zone including the macroscale description of large and small SSEs, the mesoscale characterization of the transient slip dynamics on the rupture surface during an ETS episode, and finally the nature of rapidly repeating failures of individual LFE clusters. The spectrum of geophysically visible ETS behavior ends at the scale of individual LFE failures with 100s of m dimension, which is larger than a typical outcrop examined by geologists. Nonetheless, interesting connections can be made between the properties of observed ETS failures and the geologic analogs.

(i) Macroscopic: Large-scale SSE characteristics

Inversions of geodetic measurements allow for characterizing the macroscopic dimensions, slip and other kinematic source properties of large-scale ETS events. One outstanding feature of these SSEs is the minute amount of slip (few cm) that even the largest (> 100 km along arc extent) events accommodate (Table 2). Given the small amount of slip, similar-sized ETS events frequently recur every few months to a couple of years, and thus many dozens of events have now been observed in the well monitored subduction zones in Cascadia and Japan. The small slip also means that the ETS events have very low stress drops of < 100 kPa, compared to the 1 - 100 MPa range of regular earthquakes. SSEs in the tremor-producing zone appear to be limited to a seismic moment equivalent to Mw 6.7, slowly released over the course of a few-weeks-long episode. However, in some subduction zones much larger (Mw > 7) long-term SSEs extend into the generally aseismic zone between the ETS zone and locked sections of the megathrust, which can endure for up to several years [59–62]. Consideration of the spatio-temporal patterns in the distribution of tremor and LFEs resolves low-magnitude SSEs associated with smaller tremor bursts that are not resolved by geodetic observations alone [55,60,75].

In addition to their small slip and low stress drop, ETS stand out by the slow propagation (∼10 km/day) of their primary slip front and thus long duration of their rupture (Figure 4a). The apparent ease of growth and frequent repeat of such large-scale failures suggests a very effective means of stress communication and slow rupture propagation. Like regular earthquakes, ETS have a nucleation zone from which they often propagate up dip and then either bilaterally or unilaterally along strike of the subduction zone [55,63,77]. While the along-arc propagation of the main slip front is slow, slip-parallel migrations of tremors propagate both updip and downdip hundreds of times faster (30 - 200 km/h). This might involve interaction of the slowly laterally migrating slip front with slip-parallel linear structures on the fault or rapidly propagating fluid pressure pulses along structural features elongated in the dip direction [67,69,77]. In some cases, the nucleation and growth of ETS can be rather complex. [70] consider a 2013 ETS in which tremor and GPS data suggest initial nucleation in three different spots followed by growth and coalescence, over the course of three weeks. As the three slip fronts approach each other and merge, the rate of moment release substantially increases, suggesting that coalescence of multiple

For Peer Review Only

This manuscript has not yet undergone peer review

Table 2. Summary list of relevant source properties of episodic tremor and slip (ETS) events and low-frequency earthquakes (LFE) from geodetic and seismological constraints

Parameter	Constraint or Observable	Typical Values and Notes	References
ETS Events			
SSE rupture dimensions	tremor locations and modeling of geodetic data	From few km (tremor only) up to 10s km wide by 100s km long	[55–58]
slip per event	Geodetic inversion and tremor calibration	mm to few cm (long-term SSEs, generally extending up-dip of ETS zone, up to 10s of cm [59–62]	[56–58]
Mw	Geodetic inversion (events <~Mw 5.5 are difficult to detect)	Mw 5.3? – 6.7 (long-term SSEs may have M >>7 [59–61]	[57,58]
Stress drop	Geodetic inversion	1 – 100 kPa	[?,58]
duration		days to weeks (long-term SSEs may endure for years) [59–61]	[56,60,63,64]
recurrence interval		months to years	[47] and refs. cited therein
propagation velocity	tremor/LFE space-time distribution	along-strike: 5-15 km/day along-dip: 30 - 200 km/h back-propagating: 5–20 km/h	[63,65–69]
slip rate	Geodesy/tremor	1-2 mm/day	[14,58,70]
rise time (duration of slip at a point on the fault)	Geodesy/tremor	5-30 days	[56]
LFEs			
rupture dimensions	Seismic waveforms	0.1 - 1 km	[13,71]
slip per event	Seismic waveforms, number of LFEs per ETS	0.05-0.12 mm (if multiple distinct slip patches contribute to LFE-family failures, slip could reach few mm) [13,72]	[13,71,73]
Mw		1-2.5	[71,73]
stress drop	Seismic waveforms	1-10 kPa for 1 km patch size (if dimensions are 0.1 km, stress drops can reach 1 MPa) {Chestler, 2017 #3364}	[13,71,73]
duration		0.2 – 0.7 s	[71,73]
recurrence interval (in "LFE family")		seconds to days	[74,75]
rupture velocity		~0.7 km/s	[73]
slip rate		~0.25 mm/s	[73]

For Review Only

rspa.royalsocietypublishing.org Proc R Soc A 0000000

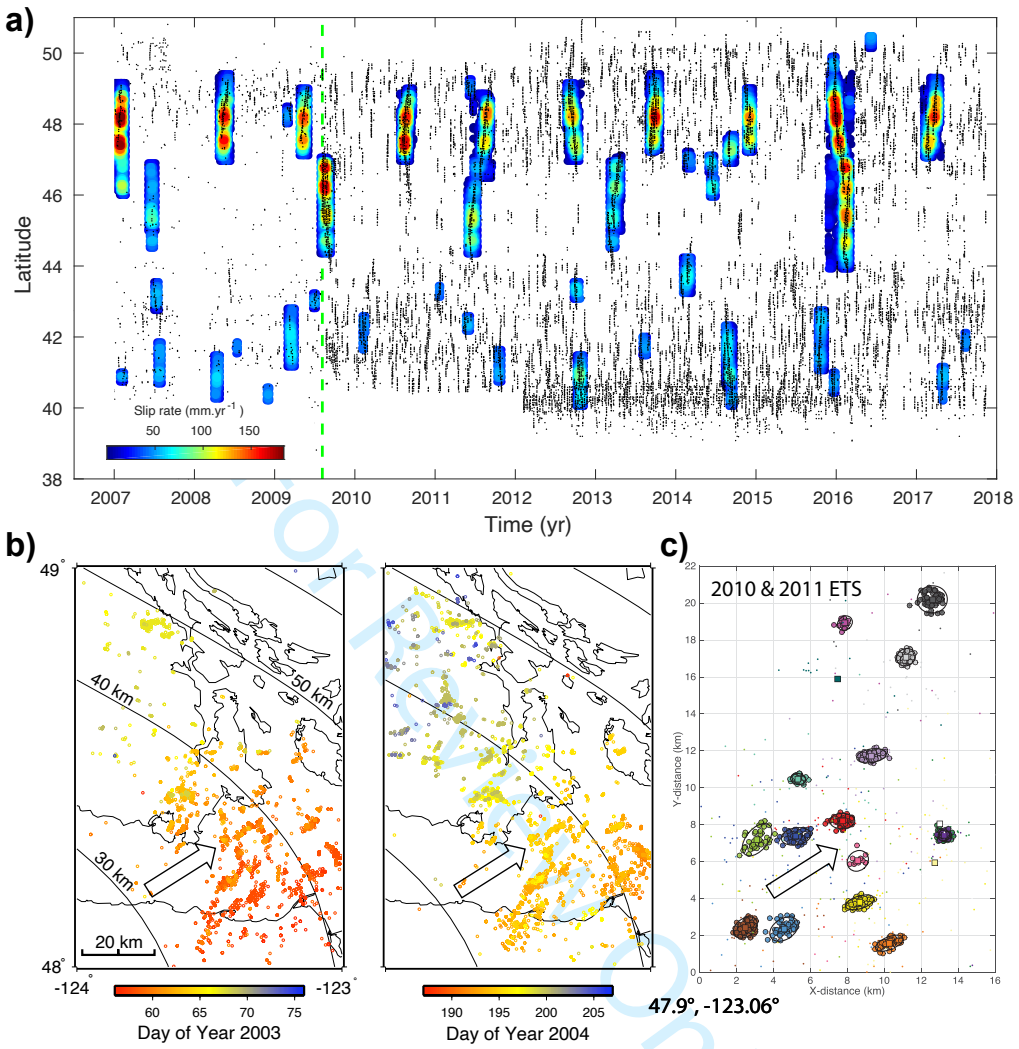

Figure 4. Geodesy and source seismology illuminate the hierarchy of ETS and LFE on Cascadia subduction zone. (a) Spatio-temporal distribution of slow slip events (color contours indicating slip rate) and tremors (black dots) along the ETS zone of Cascadia (based on [58]). (b) Spatio-temporal distribution of tremor sources during two ETS events in northern Cascadia. Tremor clusters light up many of the same source patches in recurring events (based on [76]). (c) LFEs clustered in LFE families that failed during two ETS in 2010 and 2011 (also shown in (a)) (based on [13]. Open arrows in (b) and (c) indicate the plate convergence direction.

ETS can lead to a more energetic event [70]. [75] evaluate the slip evolution of a long-term SSE inferred from GPS time series and LFE recurrence intervals in the ETS zone at Guerrero to develop a conceptual model of updip migrating pore-pressure pulses modulating the slip and strength of the fault zone. As the up-dip SSE develops and loads the LFE source region, slow slip accelerates in the ETS zone. Increased anisotropic permeability leads to up-dip fluid pressure diffusion and a transient decrease in pore pressure, and thus a pronounced deceleration of LFE activity down dip to below inter-ETS levels, even as the long-term SSE continues. This case study supports the idea that fluid pressure cycles and fault valve behavior controls the spatio-temporal distribution of slip in the ETS zone.

This manuscript has not yet undergone peer review

As pressure, temperature, permeability, and other conditions and properties vary both in the down-dip and along-arc direction, there is interest in resolving systematic effects of such parameters on the ETS behavior [47]. [55] use the tremor activity in Cascadia to find a systematic decrease in size and increase in frequency of events with increasing depth. A similar first-order transition to more episodic slip behavior is found in the Nankai subduction zone and in Mexico [75,78]. While [55] put forward a model invoking a cascading stress transfer process, [47] suggest that the systematic decrease of recurrence interval with depth is governed by temperature dependent silica precipitation and healing processes, which reduce fault zone permeability and thus accelerate overpressure development and shorten the time to the next ETS failure. [79] carry out a systematic analysis of changes in the temporal clustering of tremors to evaluate such spatio-temporal patterns in tremor sequence duration and recurrence intervals in a handful of global tremorgenic subduction zones, finding both downdip and lateral variations. More such comprehensive explorations of variable ETS behavior in the context of varying ETS zone conditions should improve our understanding of the underlying mechanics and hydrology of the ETS phenomenon.

(ii) Mesoscale: Spatio-temporal tremor distribution and ETS slip variability

The distribution of tremors in space and time provides detailed information about the structure and dynamics of ETS. It appears that tremor sources persistently illuminate many of the same patches in the recurring ETS events, suggesting inherent structural or lithological differences in the tremor-producing portions of the SSE rupture. [80] highlights apparent alignments or striations in the tremor source distribution in Japan, which appear to align with the direction of plate motion but also past plate convergence directions. This suggests that the striations reflect plate interface structures that could have developed by subducting plate structures. Similarly, [76] show that the same clusters of LFEs light up in repeated ETS, suggesting that these are persistent features of the plate interface (Figure 4b).

Once the main slip front of an ETS rupture has passed, dynamic bursts of tremor activity [63,68] and slow slip [81] continue in its wake, for many days. During this period, coherent migrations of LFEs and tremor on slipping portions of the fault are observed, suggesting secondary slip transients with a range of dimensions, propagation speeds and directions, moments, stress drops, and other characteristics [77,81,82] [68,69,77,83]. The secondary slip fronts start within about 1 km of the main tremor front, and propagate at variable rates backwards, forward and parallel to the main front [77,83]. [83] used cluster analysis to catalog more than 1000 of these secondary tremor and LFE migrations contained in Cascadia ETS, lasting up to ~30 hours, to systematically inventory their source properties. They find that short-duration secondary slip fronts dominantly propagate along dip while the more enduring ones mostly propagate along strike. Peng et al. [68] find many smaller-scale subevents propagate at 10-60 km/h right behind and parallel to the main front of tremor migration, which may or may not be aligned with the dip direction. They thus conclude that even though the ETS zone may have a slip-parallel anisotropic fabric it does not control the orientation of the main front or strongly influence the migration pattern of the secondary fronts. The larger-scale and somewhat slower tremor migrations occur further behind the main front and appear to continue across portions of the fault without many tremor sources [63,68]. These later migrations advance at 10–20 km/h [63,69], 25–50 times faster than the main SSE front, and their slip is faster by a similar ratio. As opposed to the initial set of secondary tremor bursts, events in these larger-scale secondary tremor migrations are strongly tidally modulated [84]. The tidal sensitivity increases over the course of several days, suggesting that the fault weakens as ETS slip grows [85]. Thus it appears that some aspect of the ETS faulting process limits the main slip front growth and speed but permits the secondary fronts to propagate and slip faster and to weaken and become increasingly sensitive to tidal stress.

For Review Only

(iii) LFE source characteristics

LFEs are small seismic events contained within tremor, first recognized by [86] in southwest Japan. They represent barely observable seismic signals extracted from continuous waveform data, which are characterized by lower frequencies (> 1Hz) and longer durations (0.2-0.5 s) than those observed for ordinary microearthquakes [87,88]. It is possible that localized, near-source attenuation of seismic waves, which may be the result of high pore-fluid pressures and rock damage in the LVL, could cause the bandlimited nature of LFEs through the depletion of high frequencies [89,90]. LFEs with a maximum size of about Mw 2.5 have approximately constant durations and appear to break asperities of similar dimension (1 km), suggesting that moment variation is dominated by differences in slip [71]. LFE focal mechanisms and polarizations are consistent with a double-couple source, originating from areas in the plate interface that are stationary in space and persist for decades [76,91,92].

An important characteristic of LFEs is their repetitive nature; each LFE source in space (LFE family) can generate hundreds of events during each ETS, interpreted as either the repeat failure of a single asperity or adjoining failures within a relatively tight cluster of asperities (Figure 4c) [5,13,15,74]. Recurrence intervals in a family during an ETS can be as low as a few seconds. Such rapid repeat failures challenge standard models of failure cycles involving healing and restrengthening of a slip surface. [13] argue that each LFE family typically hosts multiple separate patches (Figure 2b). Thus, while estimates of slip per LFE are on the order of 0.1 mm, assuming single-patch failures [13], slip could reach a mm if there are ∼10 patches in a family and more if those patches are spatially separated in a ductile matrix [13] (Figure 2b). Stress drops are thought to be ∼10 kPa [71,73], but [13] suggest that stress drops could be up to 1 MPa, getting close to values for regular earthquakes, if LFEs in a family have smaller slip areas and are more spaced out on the family patch (see Figure 4c). Given that geological observations indicate that subduction thrusts have finite thickness increasing with depth (see below), the LFE families could also be distributed in a three-dimensional volume of ductile material, thus allowing for less slip and lower stress-drop per LFE [13]. LFEs and tremor only release a tiny fraction (∼0.1 %) of the otherwise aseismic plate-interface slip in the ETS zone [13]. This suggests that LFE family clusters represent small areas in the fault zone that are mechanically distinct from their aseismically shearing surroundings, representing local anomalies in lithology, metamorphic assemblage, fluid pressure, and/or permeability.

In addition to LFEs, distinct very low frequency earthquakes have been detected in broadband seismic records at even lower frequencies of 0.02–0.05 Hz [93]. Occurring within tremor zones, both deep and near-trench, they seem similar to LFEs and are also the result of shear slip on the plate interface, but they have longer durations (10–200s) and larger magnitudes (M 3–4) [10,94]. While many of these more enduring slow earthquakes appear to be contained in tremor sequences, they can occur independently, separated from tremor in both space and time [95]. Even though these very low frequency sources appear to be clearly distinguished from LFEs, [96] suggests that this separation is potentially an artifact of Earth's microseism noise hiding signals in the intervening frequency range (0.05–1 Hz). Thus the different seismic and aseismic slip phenomena observed in the ETS zone may be parts of a common broadband slow slip process [18,96]. Improved seismological and geodetic observations with higher spatio-temporal resolution and over a broader frequency range would help resolve further details of the complex slip behavior in the ETS zone.

(c) Scaling and Probing the Mechanical Properties of ETS

To better understand the underlying mechanics of slow slip and regular earthquakes, there has been much interest in the scaling relationships of SSEs, in particular that between their moment and duration [58,80,97]. Ide et al. [80] suggest that the moment of SSEs scales linearly with their duration over a wide range of scales from individual LFEs to the largest ETS events. This is in contrast with the systematic duration-cubed scaling of regular earthquakes. However, several

For Review Only

This manuscript has not yet undergone peer review

recent studies [58,62,64] find that such a systematic difference does not hold when considering SSEs from a particular environment or of a different type. Thus, ETS, secondary slip migrations, very low frequency earthquakes, LFEs, and regular earthquakes may all feature similar, pulse-like rupture propagation and their rupture velocities and stress drops vary with the size of the event. Nonetheless, there is a large and real gap in detection of fault slip processes between the two proposed scaling relationships for SSEs and regular earthquakes, suggesting that earthquakes and slow slip phenomena are two distinct fault slip processes that seem to indicate a different geological context [82]. More quantitative studies of scaling relations of SSE across their full spectrum are needed to improve our understanding of similar and dissimilar dynamics of slow and fast ruptures under different conditions.

Evidence supporting the idea that fluid pressures are very high, stress levels are low, and faults are frictionally weak in the ETS zone comes from observations of triggering of slow slip and tremor by seismic waves and Earth's tides [17,84,94,98–102]. Tremors are quite easily triggered and their amplitude modulated by few-kPa shear stress cycles from passing surface waves of remote earthquakes [17,98,99]. Similarly small tidal shear-stress changes produce substantial modulation, while the normal-stress cycles produce a more modest response, interestingly indicating raised rates during times of increased fault-normal compression [102]. The tidal shear-stress response appears consistent with rate-dependent friction at extremely low effective normal stress, whereas purely aseismic shearing of various mineralogies and power-law or exponential viscous deformation mechanisms does not appear to allow for driving such a response [103]. Considering an undrained fault model, Beeler et al. [104] suggest that the observed tremor response reflects low intrinsic friction, low dilatancy, and lithostatic pore fluid pressures. Houston [85] finds that the modulation of tremors becomes stronger as slow slip accumulates during an SSE. This indicates that the plate interface has an intrinsically low dynamic friction coefficient (< 0.1), is at near-lithostatic fluid pressure, and further weakens during continuing slow slip associated with secondary slow slip fronts [85]. Examination of tidal modulation of individual LFE families shows strong spatial variability in the correlation with tidal stress in addition to systematic temporal changes in which tidal correlation increases with time during secondary slip fronts and transitions from correlation with stressing rate to correlation with stress amplitude [102]. These studies show that detailed examination of the response of tremors and slow slip to very modest external stressing cycles allows for characterizing laterally heterogeneous and time-dependent physical fault-zone properties.

3. Geologic Observations of ETS Environment and Source

Subduction complexes exhumed from depths similar to the ETS source region (~25-50 km) occur on several continents and in a wide range of tectonic settings (Figure 1) [105–107]. Around the circum-Pacific, rocks from this source depth are dominantly oceanic in affinity and crop out in the inboard parts of long-lived accretionary prisms [108–112]. Within the Mediterranean orogens, several exhumed subduction complexes occupy the footwalls of large-scale metamorphic core complexes, and consist of intercalated oceanic and continental-affinity rocks representing subduction of rifted continental fragments and intervening small ocean basins [113–115]. Several oceanic-affinity subduction complexes also crop out in the internal zones of continental collision zones (e.g. the Alpine-Himalayan mountain belts), recording early stages of oceanic subduction and accretion prior to continental collision [116–118]. The mechanisms of exhumation of these subduction complexes are debated, but likely involved some combination of buoyancy- or pressure- driven return flow along the top of the subducting slab, and upper plate extension driven by surface elevation gradients or slab rollback [110,119–121].

Relating features preserved in these subduction complexes to processes in the modern ETS source region has several challenges. These include firstly that subduction complexes exhumed from this depth range are too deep to be exhumed simply by erosion, and instead always involve some tectonically-driven exhumation process. In many cases, the exhumation path is along a warmer geothermal gradient than the prograde path, so subduction-related structures

and metamorphic relationships can easily be obscured. Secondly, even where exhumational overprinting is weak, individual packages of rock within these complexes record subduction and tectonic accretion over several million to tens of millions of years, thus aggregating deformation over much longer timescales than individual SSEs. Thirdly, there are debates as to whether the rocks we see exhumed to the surface are representative of "average" subduction zones. van Keken et al. [122], for example, suggested that exhumed blueschist-eclogite terranes may reflect only young oceanic lithospheric slices based on a data compilation by Penniston-Dorland et al. [105] indicating that rocks were hotter than thermomechanical model predictions. A more recent compilation by Agard et al. [106], however, shows good agreement between models and P-T trajectories of recovered rocks.

Despite these challenges, there are subsets of the global array of exhumed subduction complexes that overlap in PT conditions, and that preserve both transient and long-term deformation features that may correlate to the ETS source region and process. Studying these exposures can provide key insights into a) the rock types that occupy this depth range on the plate interface and potential sources of rheological heterogeneity, b) steady-state and transient deformation mechanisms and modes, c) effects of metamorphic reactions, and d) fluid migration patterns and permeability. Here, we summarize some of the primary insights into the ETS source region and mechanisms that have been or can be gleaned from studies of exhumed rocks.

(a) Materials in the ETS Source Region and their Significance

Exhumed subduction complexes tell us which rock types make it to the deep subduction environment without being scraped off in the shallow accretionary prism; and simultaneously, which rock types become stranded on the deep interface rather than subducting ultimately into the mantle. The process that strands rocks at these depths is referred to as tectonic underplating, which is the progressive transfer of material from the down-going slab to the upper plate and the associated down-stepping of the plate interface into deeper and deeper levels of the slab [110,123–125]. Geologic observations of deeply exhumed subduction complexes indicate that sediments, oceanic crustal slices, and mantle slivers are all capable of becoming underplated at and around the ETS source depth (Figure 5).

Sedimentary protoliths involved in oceanic subduction shear zones typically include cherts, shales, greywackes, and pelagic carbonates [128], metamorphosed with progressive subduction to produce schists with variable quartz-mica ratios, meta-cherts (quartzites) and marbles, respectively. Metasediments are more abundant in exhumed subduction complexes than expected for their predicted thicknesses on the seafloor, suggesting the deep subduction interface is an important sediment reservoir due to the underplating process [106,129]. The presence of these metasediments has implications for ETS, including that a) they may help explain the correlation between ETS and the LVL [33,40,130], b) they provide an important source of fluid compositions not present in volcanic oceanic crust [131–133], and c) they are generally rheologically weaker than their mafic counterparts [121,134,135].

Oceanic crustal slices are also commonly preserved in deep subduction complexes, with protoliths that include both highly altered and pristine seafloor basalts, as well as intrusive oceanic crustal sequences such as sheeted dikes and gabbros [31,136]. These suggest that various depths of oceanic lithosphere become entrained or sliced off during progressive subduction [123,137,138]. Despite these protoliths all being similar in bulk composition (i.e., mid-ocean ridge basalt), their rheological properties on the subduction interface may change drastically as a function of initial sea-floor alteration, and metamorphic grade. Originally fine-grained, altered basalts, for example, are often tightly folded with pelagic metasedimentary cover sequences on the deep interface (e.g. Figure 6), whereas originally coarser-grained gabbroic or unaltered basaltic lenses are more typically incorporated as boudinaged blocks and/or underplated as intact slabs, especially when they have been eclogitized (Figure 7) [139–142]. The intact oceanic crustal fragments may be important for ETS because they may correspond to multi-kilometer-scale lineaments or smeared 'asperities' on the plate interface that could guide migrating slow

For Review Only

This manuscript has not yet undergone peer review

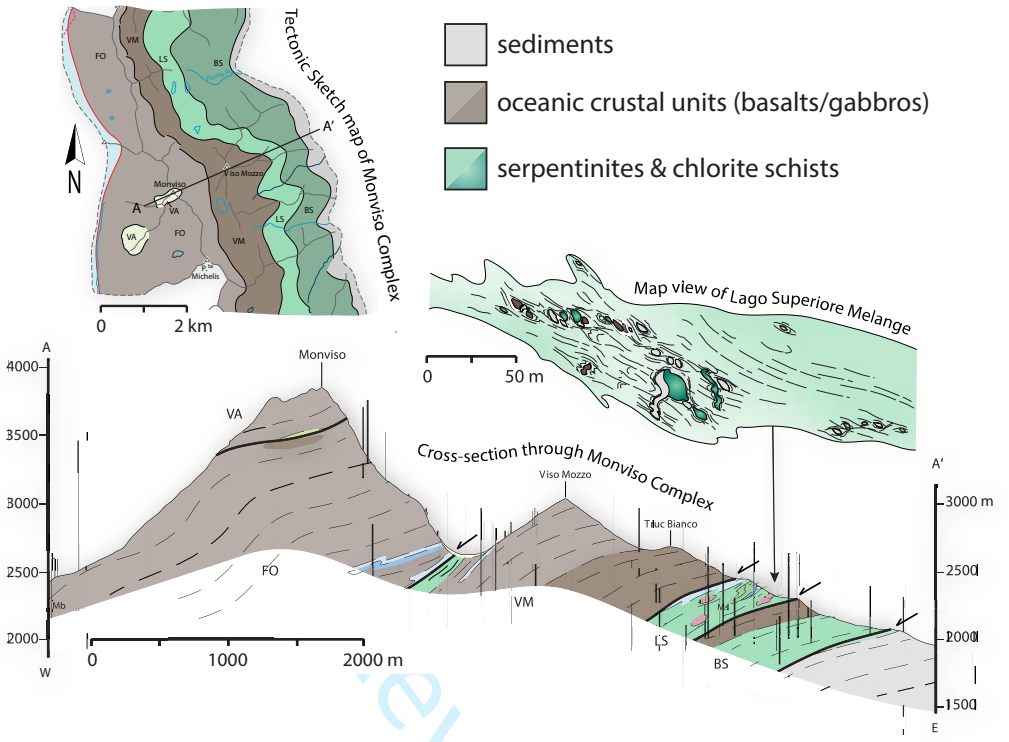

Figure 5. An example of a subducted, underplated and exhumed mafic-ultramafic complex associated with Tethys oceanic subduction preserved in the Western Alps. The complex consists of several slices of basaltic and gabbroic oceanic crust separated by high strain serpentinite and chlorite schist melange shear zones. The melange zones contain blocks of metasediments, eclogite-facies and lower-grade metabasalts, and serpentinized peridotites, representing imbricated slivers of oceanic crust and mantle. Tectonic sketch map and cross section modified from [126]. Map view of Lago Superiore melange modified from [127]

slip fronts or tremor bursts (e.g. [67,143,144]); they may also act as permeability barriers once accreted to the upper plate (cf. Section 3(d) and Figure 12).

Mantle peridotite slivers (typically serpentinized) are preserved in relatively small volumes in deep subduction complexes and have three potential sources: the down-going slab, supra-subduction zone ophiolites derived from the shallow forearc, and deeper mantle wedge material derived from beneath the upper plate Moho. Derivation from the down-going slab may relate to fracture zones or to abyssal peridotites already exposed on the seafloor, suggesting slow mid-ocean-ridge spreading environments and oceanic core complexes [145,146]; or it may imply especially deep slicing into the down-going slab during underplating [138,147]. Derivation from supra-subduction zone forearc ophiolites or deeper upper plate mantle wedge requires a subduction erosion environment, characterized by entrainment of upper plate material into the subduction shear zone, and usually indicates low sediment supply and/or variations in slab topography [148–151]. The observation that mantle slivers may be incorporated into the subduction shear zone near the trench is important to understanding ETS because it implies that ultramafic rocks can be involved as a dehydrating source rock, a weak rheological heterogeneity, and/or a fluid channel or barrier at even shallower depths along the plate interface than the mantle wedge corner.

(b) Deformation Styles and Mechanisms on the Deep Interface

rspa.royalsocietypublishing.org Proc R Soc A 0000000

(i) Long term deformation patterns

The subduction, underplating and exhumation histories, and the temperatures around and above the brittle-ductile transition within deep subduction complexes, mean that the majority show distributed, polyphase ductile deformation to very high strains. It is common for even the simplest exhumed rocks to preserve three deformational fabrics, including: 1) an early prograde fabric cryptically preserved in the cores of later folds and/or as inclusion trails in metamorphic porphyroblasts (e.g. garnet), 2) a penetrative fabric formed at near-peak metamorphic conditions, and 3) a variably developed overprinting fabric produced during later exhumation (e.g. [152–156]). The transitions from one fabric to another is often accompanied by changes in kinematics, including tectonic transport direction and/or strain geometry (e.g. [152,157]). Rocks deformed in this distributed ductile manner on the subduction interface can form coherent tracts, continuous across multiple lithological boundaries and previous tectonic contacts (e.g. thrust faults), suggesting that over long timescales the plate interface can be several kilometers in width (Figure 6). Even where these coherent terranes have escaped exhumational overprinting, they represent deformation integrated over a minimum of ~0.5 million years (based on maximum subduction rates and slab dips). At these timescales, bulk deformation is accommodated by viscous flow in the weaker subducted units, involving both pressure solution (most common in metasediments and fine-grained mafic rocks) and dislocation creep (in some mafic rocks or quartz-rich metasediments and veins) [158–162]. Where shear stress magnitudes have been estimated from recrystallized grain size piezometers in quartzites and/or from experimental flow laws, they are under ~10 MPa [159,163–167]. These long-term deformation patterns are relevant to understanding the ETS source region firstly because they reflect deformation processes that dominate over many earthquake cycles, and secondly because of the frozen-in seismic velocity/anisotropy signals they store along the plate interface, which can remain long after the active subduction interface has migrated structurally downward.

(ii) Transient deformation patterns

In making comparisons to the ETS source region, we are interested in detecting transient deformation signals embedded within the integrated subduction history described above. We distinguish these features in the rock record as spatial changes in deformation mode, from distributed ductile flow, to synkinematic fracturing, frictional sliding, or accelerated viscous creep, which implies a local switch to strain rates elevated above the background steady state [168–174]. There are two key challenges in interpreting these features, however. Firstly, *how* elevated the strain rates were is very difficult to quantify from the rock record [175], although some estimates can be gleaned from correlating deformation mechanisms in the rocks to experimental flow laws. The "smoking gun" for recognizing seismic strain rates is pseudotachylite (but see [176] for a summary of other potential indicators of seismically-generated frictional heating). Pseudotachylite is described for only one of the 30-50-km-deep subduction interface localities shown in Figure 1 (Corsica, [177]), whereas they are described for a handful of subduction complexes exhumed from the shallow subduction interface (e.g. [178–181]). This may imply that fast seismic slip along the deep interface is rare, consistent with seismic observations of modern subduction zones. However, the generation of frictional heat is sensitive to both the velocity of slip and the shear stresses, so their absence does not rule out the possibility of seismic slip on the deep interface where shear stresses may generally be very low. The second challenge is that transient deformation features are bound to be only minimally preserved because in many places they are erased by the longer-term aseismic creep process (cf. Figure 6).

One of the most widely documented potential markers of transient deformation in subduction complexes are "melange belts", which we loosely define here as localized high strain shear zones in which blocks of higher viscosity material are embedded in a less viscous matrix [182–185]. These most commonly develop in rheologically weak geological units such as phyllosilicate-rich

For Review Only

This manuscript has not yet undergone peer review

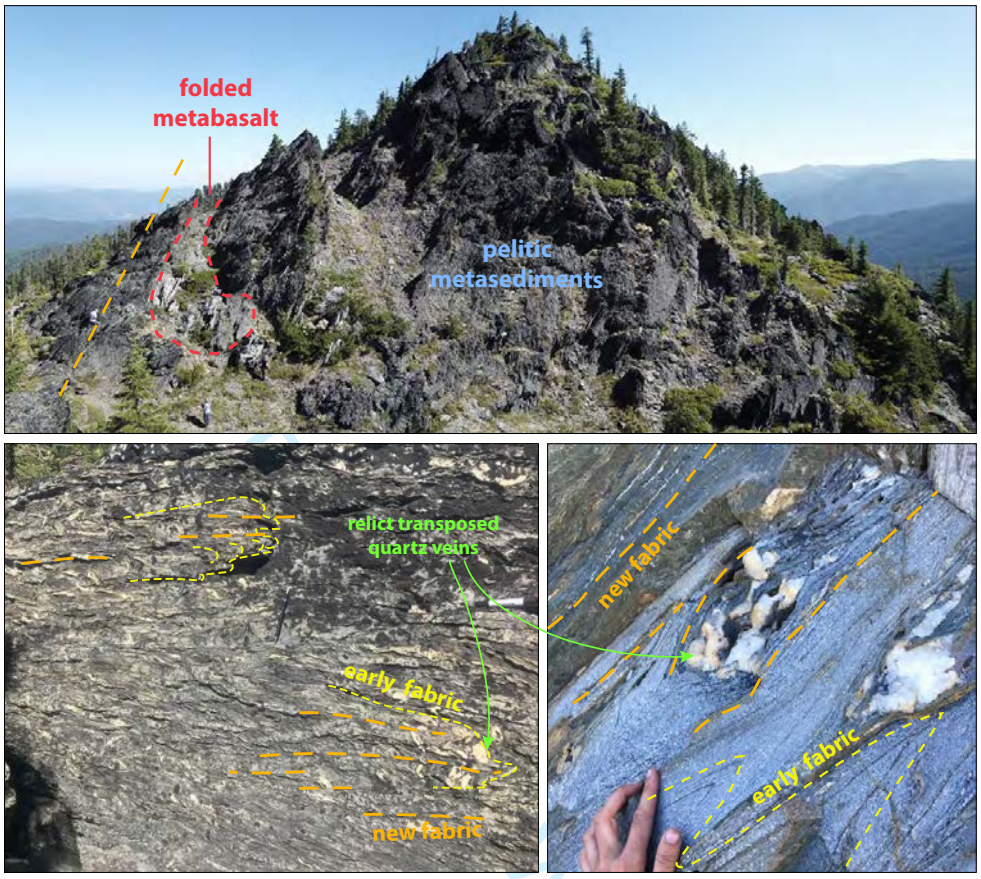

Figure 6. Example of viscous deformation patterns that accumulate over long timescales at the ETS source depth, from the blueschist-facies Condrey Mountain schist in the Klamath Mountains of northern California/southern Oregon. [A] A massif with metasediments tightly folded around a blueschist-facies metabasaltic lens, likely representing an older thrust fault contact, now transposed by distributed viscous deformation. [B-C] Graphitic mica schists (B) and quartz schists (C) showing two prograde subduction-related fabrics and several generations of quartz veins variably transposed by the youngest schistosity. While the quartz veins may have formed during transient deformation pulses, the record of this process becomes dismembered during subsequent viscous shear.

metasediments and serpentinites, and contain mafic or ultramafic slivers or blocks such as coarse-grained amphibolites, eclogites and/or relict peridotites. Experimentally-derived flow laws for this range of subduction zone materials predict viscosity contrasts of up to 4 orders of magnitude in the temperature range of ETS (400-550°C) (see compilation in Figure 2 in [135]). Melange belts are potential culprits for transient deformation firstly because they are characteristically narrower than coherent terranes, implying that they record elevated strain rates, and secondly because the deformation mechanisms they record are nearly always combined frictional-viscous creep at a variety of length-scales [169,186]. That is, due to their high viscosities, the clasts within these melange belts cannot yield viscously and instead accommodate fracture and frictional sliding through veining and faulting that is synkinematic with viscous strain in the surrounding matrix (Figures 7,11). The brittle deformation in the clasts can be triggered by stress concentrations generated at clast margins and/or by transient increases in pore fluid pressures (e.g. [187–190]).

An additional possible form of transient frictional-viscous creep that does not necessarily require significant lithological variations are localized shear zones that appear to have deformed

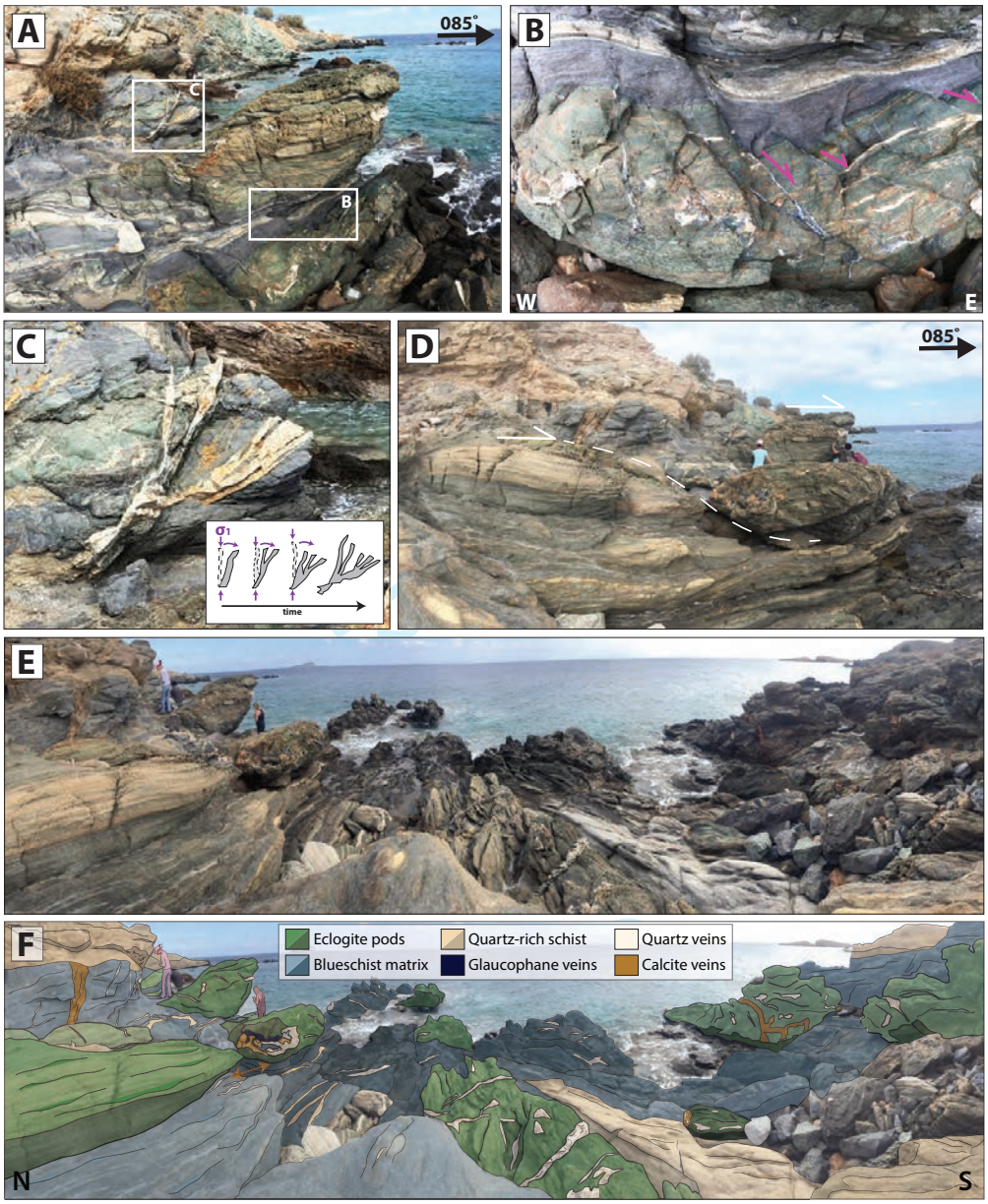

Figure 7. Examples of frictional-viscous deformation in a blueschist-facies shear zone on Syros Island in Greece, modified from [140]. [A] Lensoidal mafic eclogite pod (∼4 m in length) embedded in a blueschist and quartz schist matrix. [B] Zoom in on the base of the eclogite pod showing brittle shear veins filled with high pressure minerals (e.g. glaucophane). The brittle shear veins culminate in discrete ductile shear zones in the surrounding blueschist matrix, indicating coeval frictional viscous slip. [C] Zoom in on the flanks of the eclogite pod where several generations of quartz veins were emplaced and subsequently sheared in a top-right shear sense, indicating cyclical switches from brittle vein emplacement at high pore fluid pressures to viscous creep and back again (cf. Figure 9a). [D] Meter-scale boudinage of an eclogite lens, with the boudin neck filled with blueschist facies minerals. [E-F] Panoramic photo of the entire outcrop highlighting the distribution of brittle eclogite pods and their vein structures, within the dominantly viscously deformed matrix.

This manuscript has not yet undergone peer review

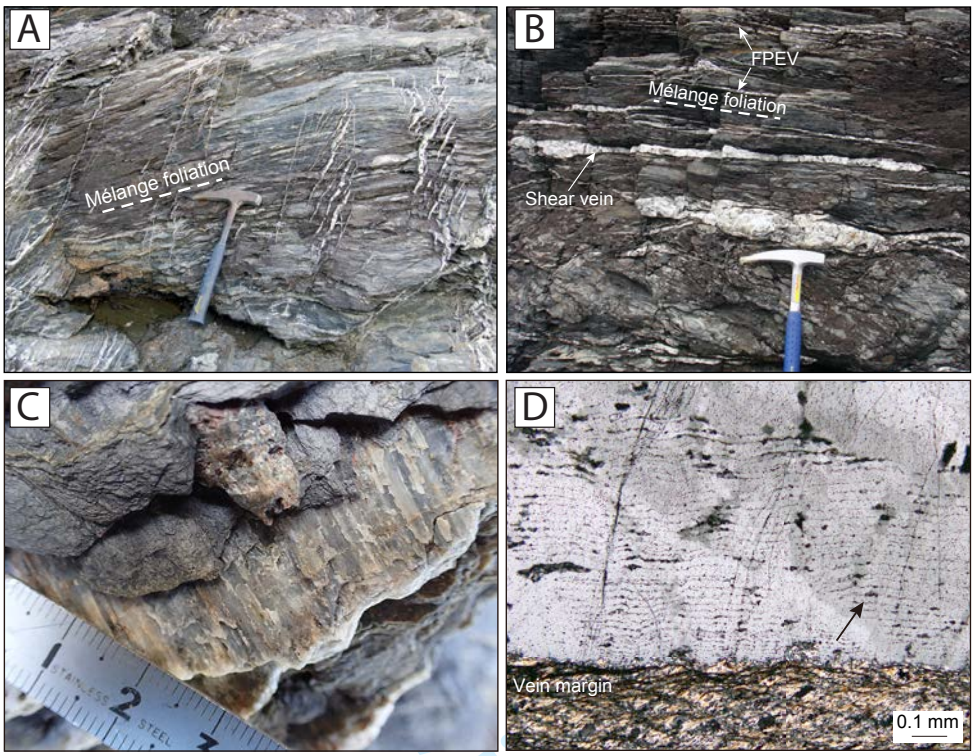

Figure 8. Examples of transient deformation features preserved in the Makimine melange in the Shimanto accretionary complex in Japan, modified from Ujiie et al., 2018. A) Mutual cross-cutting relationships between melange pressure solution cleavage and extensional shear fractures cf Figure **??**A. B) Coexistence of foliation-parallel and foliation-perpendicular veins suggesting transient switches in the orientation of sigma-1 with respect to the shear plane. C) Quartz slickenfibers developed on foliation parallel veins highlighting the shear component. D) Photomicrograph of crack-seal texture in foliaton-parallel dilational shear veins, indicating many stages of fracture opening and precipitation.

by some combination of pressure solution, frictional sliding on phyllosilicate laminae or cleavage planes, and dilational micro-cracking [191,192]. Pressure solution involves the dissolution of soluble minerals in the direction of maximum compressive stress and reprecipitation in the extension direction [193–195]. This process segregates insoluble minerals, such as micas, amphiboles and oxides, forming discrete and highly anisotropic cleavage domains, from soluble phases such as quartz precipitated in veins and microlithons at varying angles to the cleavage domains. Several subduction complexes deformed under greenschist and blueschist-facies conditions show evidence for shear slip along weak cleavage planes (e.g. [196,197]) or along kink-like micaceous crenulation bands [164] that appear kinematically linked and coeval with incremental precipitation into dilational fractures (Figures 8, 9).

(iii) Transient deformation and fluid pressures

The two types of transient deformation features described above are ubiquitously associated with evidence for cyclical variations in fluid pressures (Figure 9). Veins themselves represent tensile fractures, which require the pore fluid pressures to locally exceed the magnitude of the minimum compressive stress. The occurrence of purely extensional veins oriented at high angles to the shear fabric in these systems imply ~lithostatic pore fluid pressures and low differential stresses. It is common for the interior of dilational veins to exhibit "crack-seal" textures that

rspa.royalsocietypublishing.org Proc R Soc A 0000000

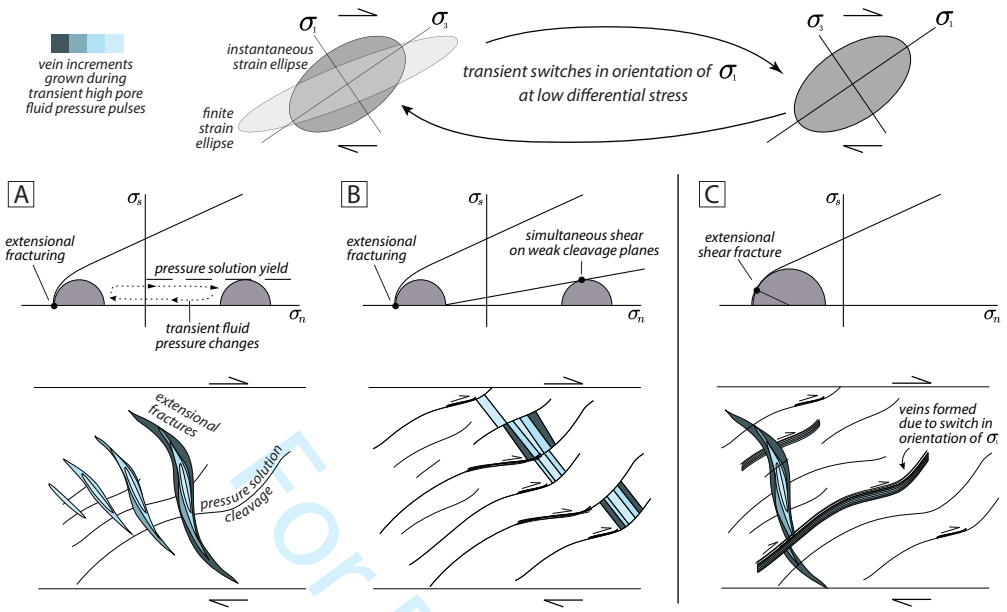

Figure 9. Examples of changes in mechanical state during transient deformation as based on vein and fabric relationships in melange belts. A) A scenario in which viscous pressure solution creep dominates long term deformation and controls the orientation of finite strain. Extensional fractures (commonly including a shear component) form during transient high pore fluid pressure pulses, and are subsequently viscously deformed and rotated during inter-event periods (see [140] and Figure 7). B) A scenario in which weak cleavage planes formed by viscous creep may evolve into shear fractures oriented at high angles to the maximum principal stress (Sigma-1) due to low cohesive strength and simultaneous high fluid pressures. These shear fractures can be activated at the same time as (and rate-limited by) precipitation into extensional veins (see [169]). C) A scenario in which there are mutual cross-cutting relationships between dilational fractures oriented at both high and low angles to the melange fabric, suggesting transient switches in the orientation of Sigma-1, also an indicator of near-lithostatic pore fluid pressures (see [197] and Figure 8).

For Review Only

reflect precipitation pulses [197–201]. In some instances these show changes in composition of the fluids at ~constant metamorphic conditions, evidenced by different mineral precipitates from the same metamorphic facies forming in a single vein over time (e.g. [143]). Additionally, in some blueschist and eclogite terranes, garnet zoning patterns appear most consistent with short-timescale growth-dissolution cycles driven by fluid pressure pulses, as opposed to long-term changes in metamorphic conditions (e.g. [202]). Even where crack-seal textures are not present, cross-cutting relationships among vein sets can show a repeating progression of vein opening, infilling, and rotation into the shear plane by ductile creep processes (e.g. Figs. 7,9a). There are also examples of mutually cross-cutting relationships between veins opened both perpendicular and parallel to the shear zone fabric, suggesting transient switches in the orientation of the maximum compressive stress, also indicative of very high pore fluid pressures (Figs. 9c, 8). These lines of evidence for high pore fluid pressures from the geology are consistent with the geophysical observation of tidal triggering of ETS events; additionally, the high fluid pressure is observed over a wide range of metamorphic conditions (greenschist to eclogite facies) and are thus also consistent with the observed high *Vp/Vs* ratios of the seismic LVL.

(iv) Transient deformation length- and time- scales

The transient rock deformation patterns showing a combination of accelerated viscous creep, and cyclical frictional deformation triggered by high fluid pressures appear to qualitatively resemble

This manuscript has not yet undergone peer review

inferences from geophysical observations of ETS. We can also attempt to make semi-quantitative comparisons of the length- and timescales of transient geologic features relative to ETS events.

First considering length-scales, geophysical data suggest the dimensions of individual LFE families is between 100 m to 1 km, and slip-per-event ranges from 0.05 to ∼3 mm. In geologic exposures, shear and dilational displacements, where recorded by offset features, vein widths, or crack-seal textures, are very similar in magnitude to LFE slip (Figure 10), suggesting they could relate to the LFE source. However, the slip area of individual veins or shear surfaces in rocks are typically < 1 m, at least one order of magnitude lower than the minimum size inferred for LFEs from seismology. However, vein sets and shear fractures do commonly cluster in discrete patches, e.g. in shear zones where high viscosity blocks, metamorphic reactions, and/or high fluid pressures are concentrated. The length-scales of these patches are more compatible with the inferred length-scales of LFEs (Figure 10). Thus, if we entertain the possibility that displacements within the patches are able to 'communicate' over the areas of their geologic exposure, estimated moments are more similar to those inferred from LFEs. Achieving moments characteristic of some of the larger geodetically-detected slow slip events would then require this 'communication' process to extend to even larger scales, linking up heterogeneous patches both along strike and up and down-dip; or alternatively, it would require heterogeneous patches of much larger dimension to exist on the deep interface such that what we see in rocks is a minimum length-scale due to the exhumation context in which we view them.

In now considering timescales, the geophysical data indicate that recurrence intervals of ETS events are on the order of months to years, whereas LFEs belonging to an ETS family recur in seconds to days, with hundreds of LFEs within each ETS event. As discussed in Section 2.2, LFE recurrence has been interpreted as either repeat failure of a single asperity, or adjoining failures within a relatively tight cluster of asperities. If, as discussed above, we interpret clusters of dilational shear fractures as the geologic record of these failed asperities, healing rate estimates become essential to quantifying likely recurrence times. In the case of block-in-matrix-type melanges, for example, vein closure can lead to restrengthening and restoration of cohesion in blocks while simultaneously causing fluid pressure build-ups due to decreased fracture porosity and permeability. And in the case of frictional shear on weak interfaces combined with dilation, the slip process itself will be rate-limited by vein precipitation. If very fast healing is assumed, then shear veins opening and closing along a single fault plane with LFE source dimensions may explain LFE recurrence and source. Alternatively, if the LFEs are sourced from heterogeneities within a 3-dimensional shear zone, then they may represent distributed dilational shear events that occur rapidly, but in different locations within a thick ETS slip zone. In the latter case, vein healing rates could more closely match the recurrence interval of ETS events, rather than individual LFEs.

Estimates of healing rates have been examined theoretically, in laboratory experiments, and via natural observations, but proposed timescales for subduction zone settings vary over several orders of magnitude. Ujiie et al. [197] used a kinetic model for quartz precipitation driven by fluid migration [203], and estimated that crack-seal textures in a low temperature (∼300C) frictional-viscous shear zone had a minimum healing time of 1.6-4.5 years, generally longer than typical ETS recurrence times. This model also predicted a fluid pressure drop of >150 MPa, much larger than the < 10 MPa estimates of [52]. Recent kinetic models inspired by natural melange shear zones by [204] examined the rates of diffusive redistribution of Si from melange matrix to blocks for two potential driving forces: 1) a transient drop in fluid pressure, and 2) a difference in mean stress between matrix and clasts. Their application of the model to geothermal gradients typical of subduction zones suggests minimum healing times of 10 to 100 years over the depth range corresponding to ETS (∼30-50 km), again much longer than ETS recurrence intervals, but perhaps more comparable to earthquake recurrence. In contrast to these estimates of annual to decadal timescales, early experiments by [205,206] suggested that crack healing in quartz can be very rapid, completed within hours at temperatures as low as 300°C. Additionally, recent work using Li diffusion modeling on transport veins in an eclogite melange block in

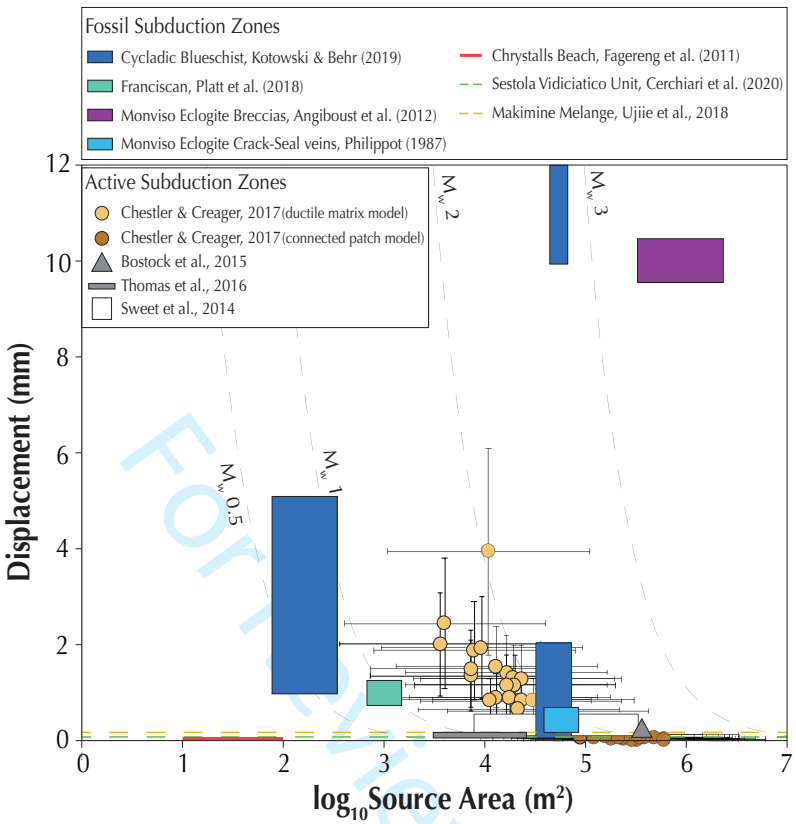

Figure 10. Comparison of source areas and event displacements from active and fossil subduction zones. Displacements from the geological record are based on the widths of crack-seal vein increments and/or measurable shear displacements within shear veins or along faults. LFE source areas and slip are based on the assumption of single-patch failures, except in the models of Chestler and Creager, which assume either 3-10 distributed sources in a ductile matrix or contiguous slip patches make up an LFE-family source area. Source areas are estimated from the mapped area of map-scale heterogeneities (e.g. mafic blocks or melange zones) resolved onto a plane oriented parallel to the dominant subduction foliation (cf. [140]), or from estimates of the length of planar faults or shear zones as described by the authors (in which case equal length and width dimensions were assumed). In some studies displacements were reported but information on possible source area could not be gleaned– these are plotted as dashed horizontal lines.

New Caledonia suggested vein precipitation occurred in 1-4 months [207]. More estimates like this from experiment and natural observation will ideally help calibrate theoretical models and provide more insight into links between vein precipitation and ETS phenomena.

(c) Geologic Constraints on the Role of Metamorphic Reactions

The depth estimates discussed in Section 2, coupled with the modeled geothermal gradients in modern subduction zones that host ETS events suggest that the ETS source spans the upper greenschist through blueschist and into lower pressure eclogite and high pressure amphibolite facies for sediments and mafic rocks, and antigorite facies for serpentinized peridotites in the mantle wedge [208]. There are many metamorphic reactions within this range of conditions, several of which involve dehydration and volume reduction [209]. We distinguish two timescales over which these reactions can influence transient deformation patterns that could correlate with seismic phenomena, including ETS.

For Review Only

This manuscript has not yet undergone peer review

Firstly, reactions themselves can generate instantaneous shear instabilities due to liberation of water [210] [211] and/or precipitation of new unstable phases [212,213]. Breakdown of lawsonite and antigorite serpentine, two phases expected to be present in the ETS source region, are especially well-studied examples that exhibit instantaneous 'dehydration embrittlement' in laboratory experiments, defined by the development of localized fault planes and/or acoustic emissions [214–218]. Additionally, reaction kinetics experiments on lawsonite and antigorite indicate these reactions are rapid, inducing high fluid discharge rates on the order of 10^{-5} to $10^{-8}s^{-1}$ (e.g. [219] (Daniel et al., 2013), which is 1-5 orders of magnitude slower than estimated strain rates of viscous relaxation (10^{-9}-$10^{-11}s^{-1}$) (e.g. [220]), supporting the idea that dehydration can lead to instantaneous hydrofracture. These reactions have been implicated in both intermediate depth slab seismicity [215,221] and as possible contributors to ETS [208,222–225].

To identify instantaneous dehydration embrittlement in the geologic record, we would look for transient deformation features (i.e. highly localized shear zones) in close association with the mineral reaction products. Interestingly, examples of shear instabilities associated directly with lawsonite dehydration reactions in exhumed rocks have thus far not been documented. There are in fact several descriptions of pristine lawsonite pseudomorphs formed on the prograde path with no evidence for closely associated brittle faulting or localized shear strain ([226] [227] [228–231]). In contrast, there are a few examples of shear slip generated in close association with antigorite dehydration in the field [213,232]. Some of the best examples come from the Voltri Massif (Erro Tobbio unit) in the Italian Alps where partially hydrated peridotite bodies and serpentinite mylonites exhibit synkinematic shear bands and hydraulic fractures decorated with fine-grained reaction products of antigorite breakdown [233–235]. These may be analogs for tremor signals located in the upper plate of subduction zones near the Moho.

The observation that ETS events do not correlate specifically with a single metamorphic reaction, however, but span several of them, suggests that instantaneous shear instabilities cannot uniquely explain these events. Perhaps more compelling is the concept that reactions result in gradual precipitation of new minerals and/or gradual increases in fluid contents and pressures with increasing reaction progress and strain, eventually culminating in transient deformation pulses in the bulk rock. Evidence for this progression is abundant in the rock record and affects a wide range of rock types (and not just in subduction zones [236,237]). The progressive growth, alignment, and concentration of micas in low to medium-grade subduction interface rocks, for example, has been postulated to strongly influence megathrust seismic behaviors (e.g. [192,238]. Additionally, at the transition from blueschist to eclogite facies conditions in metabasalts, a switch from bulk ductile deformation in the blueschist to brittle deformation in eclogite is commonly observed, with newly formed lenses of eclogite exhibiting fracturing, boudinage, brecciation, and/or abundant veining (Figure 7) [143,200,239,240]. The switch in deformation mode is interpreted to reflect both a viscous hardening of eclogite relative to its blueschist precursor, and an increase in fluid pressures induced by blueschist mineral dehydration [140,143]. In rocks exhumed from conditions similar to the mantle wedge corner, where peridotites are being infiltrated by slab-derived fluids, strain commonly localizes into newly formed, narrow, antigorite shear zones (e.g. [233,241]) and in some places shows evidence for reaction-related fluid overpressures and associated frictional-viscous shear [213,224] (Figure 11).

(d) The Role of Fluid Migration and Permeability

Exhumed rocks from deep subduction environments have proven a rich data source for understanding the role of fluids on the subduction plate interface [242,243]. As discussed in previous sections, there are several prominent sources of fluids anticipated at the ETS source depth due to metamorphic reactions in both metasedimentary and mafic/ultramafic rocks, and exhumed rocks unequivocally preserve evidence for abundant fluid activity. Of particular relevance to ETS is whether the exhumed rocks preserve information about migration distances and pathways of subduction fluids, and/or spatiotemporal changes in permeability.

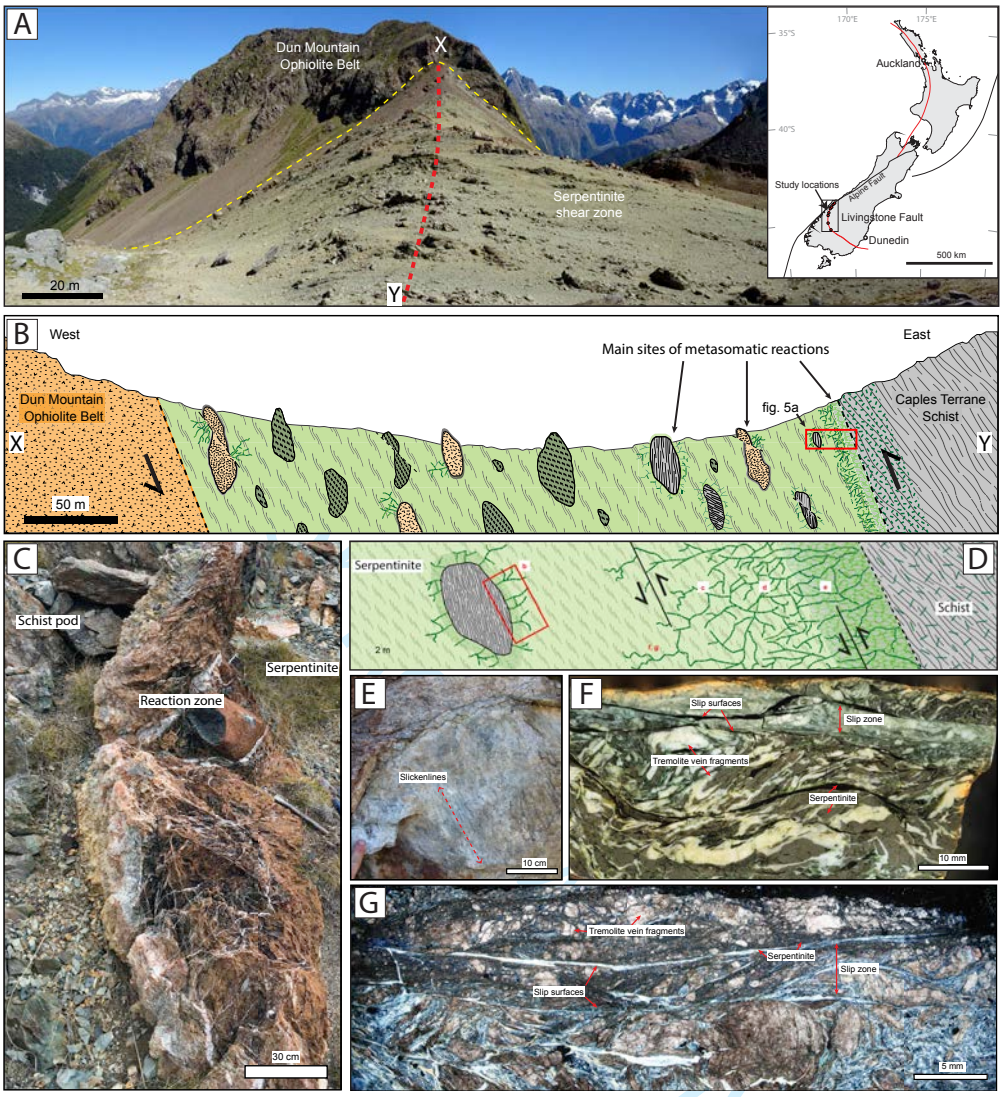

Figure 11. Images modified from Tarling et al. (2018) illustrating the interplay between chemical reactions and fluid overpressure in a mantle wedge type setting. The primary metasomatic reactions captured in this shear zone involved the addition of Si and Ca from fluids derived from adjacent metasedimentary schists, producing reaction products such as talc, tremolite, diopside and water. [A] Field photo of the 400-m-wide serpentinite shear zone associated with the Livingstone Fault in New Zealand. [B] Schematic cross section across the shear zone along profile X-Y. The shear zone contains blocks of schist (grey), massive serpentinite (dark green) and rodingite (light orange) embedded in a strongly foliated serpentinite matrix. [C] Densely veined metasomatic reaction zone adjacent to a lens of schist. [D] Schematic cross-section of metasomatic reaction zones near schist lenses and near the shear zone margin at its contact with schist. [E] Slickenlines on a frictional slip surface developed within the metasomatic reaction zone. [F-G] Polished slab and thin section showing several cataclastic slip surfaces coated with serpentinite cutting across multiple generations of folded and dismembered tremolite veins.

This manuscript has not yet undergone peer review

Given the timescales characteristic of ETS events, diffusional fluid flow processes such as grain boundary or volume diffusion are likely too slow to be relevant (e.g. [244]), so we're most interested in understanding the advection of fluids through vein networks, and along lithological contacts or shear zones, which, as discussed in Section 3.2, are abundant in exhumed subduction complexes. Both structural and geochemical observations shed light on this process. Some exhumed rocks show clear cross-cutting relationships and mineral assemblages among vein networks, such that different generations can be used to estimate the structural permeability of the rock mass under varying metamorphic conditions [173,245–247]. Muñoz-Montecinos et al. [248], for example, documented several stages of vein opening in blueschist facies rocks, and suggested they record an early stage of prograde internal dehydration, followed by hydrofracturing at high pore fluid pressures under peak metamorphic conditions. Vein textures themselves also provide some clues, with 'transport veins' showing sharp interfaces with the host rock, in contrast to *in-situ* dehydration veins, which exhibit diffusional depletion halos at their margins [243,249]. Major and trace-element data and isotopic compositions can also be used to establish whether fluids represented by veins were derived from local dehydration (implying limited transport) or from external sources (implying significant fluid transport) [242,243].

An intuitive, first-order observation that emerges from these complementary methods is that open-system fluid-rock interactions and km-scale fluid migration is much more prominent for localized high strain shear zones and melange belts than for coherently underplated mafic terranes [242,250–252]. In subduction complexes where weakly deformed slices of oceanic lithosphere metamorphosed at blueschist and eclogite facies are exhumed, for example, they dominantly show evidence for local fluid circulation and fluid entrapment [253–259], although there are some examples of fluid focusing into higher permeability transport veins [260]. Indicators of large-scale open system behavior or fluid transport into or out of undeformed mafic slabs are limited though, and the few documented examples suggest fluid migration length scales only on the order of tens of meters [261,262]. These relationships thus far imply that underplated oceanic crustal slices generally act as barriers to fluid flow on the deep interface.

In many subduction complexes, however, previously underplated and eclogitized mafic fragments become incorporated within the subduction shear zone during exhumation from eclogite through greenschist facies conditions. Once incorporated, these oceanic fragments tend to gradually lose their impermeable quality as they begin to fracture, boudinage and disperse into the shear zone matrix [250,252,263,264]. They may still retain lower permeabilities than the surrounding matrix rocks, however, and can therefore produce large spatial gradients in fluid flux, with the largest fluxes produced in the matrix adjacent to blocks with long-axes oriented parallel to the foliation [250]. Evidence for metasomatism by an external fluid source in these melange or block-in-matrix shear zones abounds. Some key indicators include: a) substantial addition of Si relative to the melange host rocks, usually in the form of multiple generations of veins of varying orientations to the shear zone foliation [247]; b) the development of reaction rinds (a.k.a. "blackwall alteration zones") around melange blocks [251,265,266]; and c) isotopic homogenization of the melange matrix [267].

The phyllosilicate-rich matrix materials that compose melange belts and subduction shear zones are also notoriously anisotropic such that these shear zones dominantly host fluid flow in the plane of the foliation, ∼parallel to the plate interface, therefore promoting fluid migration to lower pressure regions up-dip [36,268]. Experiments on antigorite serpentinite, for example, show at least one order of magnitude higher intrinsic permeability parallel to foliation than normal to it [36]. Up-dip fluid flow can also be traced in the rock record by linking fluid geochemistry preserved in veins to deeper metamorphic reactions from which the fluids were liberated. Angiboust et al., for example, used major and trace-element data from metasomatized eclogites from the Lago Superiore Unit in the western Alps to argue for ∼20-30 km of updip flow of fluids sourced from antigorite breakdown reactions downdip. Nishiyama et al. [269] recently documented high salinity, high $^{3}He/^{4}He$ fluids in strongly sheared greenschist-facies

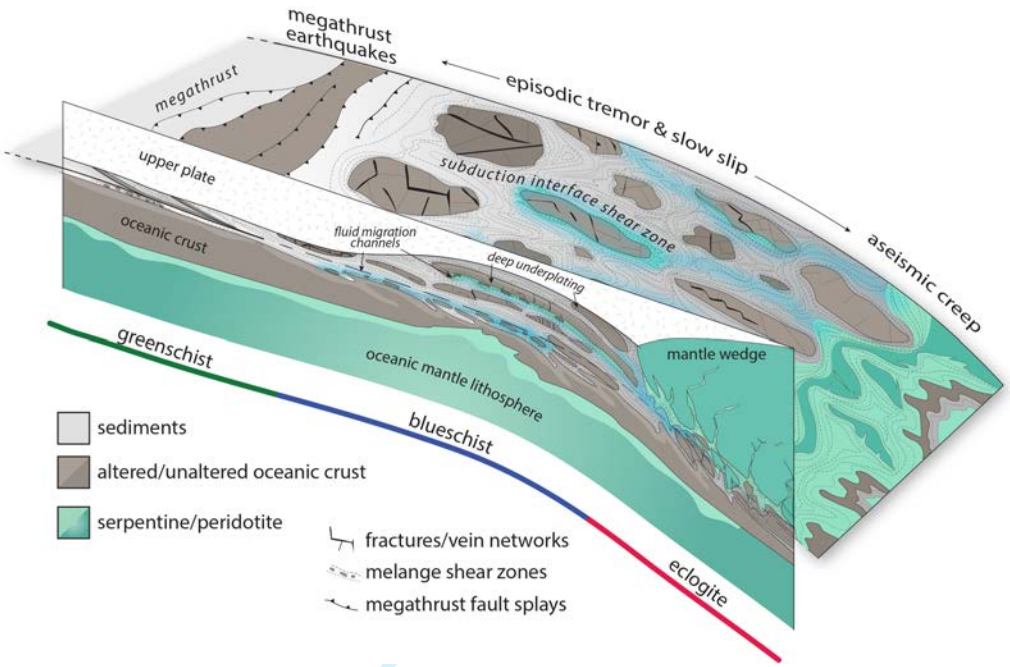

Figure 12. Summary schematic view of the subduction plate interface as inferred from the exhumed geologic record. The interface grades downward from a discrete megathrust fault and associated brittle fault splays to a wider, distributed, frictional-viscous shear zone and eventually to a zone of fully viscous shear. Through time, the active portion of the subduction interface migrates downward such that earlier subducted material is left stranded above the actively deforming zone– these underplated terranes may control the seismic velocity signatures and/or permeability structure of the broader subduction interface. The deep subduction shear zone can entrain fragments of the downgoing slab, including sediments, altered and unaltered oceanic crustal fragments, and variably serpentinized peridotite. Sediments tend to deform as broadly distributed viscous tracts over long timescales, but they record evidence for transient deformation under high Pf. Mafic rocks commonly form coherent pods or tabular lenses that accommodate transient brittle deformation triggered by fluid pressure cyclicity and stress concentrations at their margins. Serpentinized mantle material, whether entrained from the down-going slab or the upper plate mantle wedge, form high-strain shear zones that show evidence for anisotropic, up-dip fluid-flow and high fluid pressures accentuated by abundant chemical reactions. In this model of the interface, tremor and LFEs could concentrate in low vertical-permeability, frictional-viscous melange belts where fluids are trapped and rocks types are mixed. LFE migration and streaking along-dip and along-strike during ETS events could be controlled by the distribution of deformed and underplated mafic lineaments.

For Review Only

metasediments, also interpreted to represent mantle derived fluids transported updip from the mantle wedge.

4. Summary

The preceding overview of the geophysics and geology of the deep subduction interface illustrates the considerable progress being made toward understanding the structure, materials and environment of deep-seated episodic tremor and slow slip (cf. Figures 2,12). The geophysical record illuminates the close spatial and temporal relationship between low frequency earthquakes and slow slip events, the fluid-rich and high-fluid-pressure habitat that these forms of unconventional seismicity occupy, and the length-scales, timescales and mechanisms that define the ETS faulting process. The geological record strongly supports the concept of abundant fluid migration and high fluid pressures over a range of depths along the plate interface, which

This manuscript has not yet undergone peer review

may correspond well to the observations of tremor-tide correlations and the very high Vp-Vs ratios observed in modern subduction zones. Additionally, the most prominent form of transient deformation preserved in rocks from this environment involves an interplay between frictional and viscous mechanisms modulated by cyclical fluid pressure variations and defined by combined shear and vein precipitation. Although each individual transient deformation feature preserved in the rock record is small, the displacements they record, and the total outcrop areas where they are clustered scale reasonably well with inferred seismic moments of low frequency earthquakes. Key uncertainties and questions remain, however, including the following.

1) Do LFEs represent repeated (over timescales as short as minutes) rupture of small asperities on a single fault plane or are they distributed over a finite-width shear zone? In the former case, which structures would constitute these discrete fault planes in the rock record? In the latter case, what mechanisms (e.g. fluid-pressure diffusion, viscoelastic stress transfer) allow transient deformation features to communicate within a more distributed shear zone to form a coherent LFE 'patch', and to reliably participate in frequently recurring ETS events that propagate over 10s of km distances? Addressing these questions would require further improved LFE locations from geophysics, and better constraints on interface shear zone matrix rheology, fluid migration rates, and vein precipitation timescales from geology and experiment.

2) What geological processes distinguish the diverse timescales and recurrence intervals of LFEs and SSEs? What is the relative importance, to fluid pressure buildup and associated valve-like fault behavior, of processes that *generate* additional fluids (e.g. metamorphic reactions, up-dip fluid flow), versus those that *trap* fluids in place (e.g. vein closure, shear-induced permeability changes)? Improved estimates of reaction kinetics, rates of fluid flow, and rates of vein mineral precipitation could help us link these various processes to specific timescales within the diverse spectrum of slow slip transients.

3) Are the characteristics we summarize for the ETS depth range unique to the deep interface? Although we focused here on the deep interface where episodic tremor and slow slip dominates, we note that tremor and slow slip on the shallow subduction interface share many characteristics with those observed deeper. Similarly, the geologic record preserves many of the same features up dip of the locked megathrust as it does below it– e.g. wider, more distributed interface shear zones, mixed-lithology melange belts, and abundant veining triggered in this case by escape of pore waters and dehydration of clay minerals. Could slow slip and tremor simply be the 'motion and sound' of distributed, rheologically heterogeneous deformation?

4) Can the wide range of geophysical and geological observations inform the development of meaningful new approaches to modeling fault slip in the ETS zone? Ultimately, improved constraints on what's down there; i.e., the rocks, macro- and micro-structures, fluids, and reactions, need to be distilled down into meaningful fault-zone model parameters, such that we can better represent the (time-dependent) boundary conditions and geometry of the ETS system. Detailed information about the dynamic evolution of slow slip and tremor failures and their response to changing conditions and external forcing should allow for improved characterization of the spatio-temporally variable deformation, dominant deformation processes and relevant rheological properties.

Acknowledgements. The authors thank Mathew Tarling, Kohtaro Ujiie, Aitaro Kato, Ken Creager, Shelley Chestler, John Armbruster, Sylvain Michel, and Allan Rubin for providing original versions of their published images for use in this review. We thank Amanda Thomas, Pascal Audet and Allan Rubin for valuable suggestions. W.M.Behr acknowledges several helpful discussions with Alissa J. Kotowski, Carolyn Tewksbury-Christle and Miguel Cisneros.

Funding.

References

1. H Dragert.
A silent slip event on the deeper cascadia subduction interface.

Science, 292(5521):1525–1528, 2001.

2. Kazushige Obara.
   Nonvolcanic deep tremor associated with subduction in southwest japan.
   Science, 296(5573):1679–1681, May 2002.
3. Garry Rogers and Herb Dragert.
   Episodic tremor and slip on the cascadia subduction zone: the chatter of silent slip.
   Science, 300(5627):1942–1943, June 2003.
4. Thorne Lay, Hiroo Kanamori, Charles J Ammon, Keith D Koper, Alexander R Hutko, Lingling Ye, Han Yue, and Teresa M Rushing.
   Depth-varying rupture properties of subduction zone megathrust faults.
   Journal of Geophysical Research: Solid Earth, 117(B4), 2012.
5. David R Shelly.
   A 15 year catalog of more than 1 million low-frequency earthquakes: Tracking tremor and slip along the deep san andreas fault.
   Journal of Geophysical Research: Solid Earth, 122(5):3739–3753, 2017.
6. A G Wech, C M Boese, T A Stern, and J Townend.
   Tectonic tremor and deep slow slip on the alpine fault.
   Geophysical Research Letters, 39(10), 2012.
7. Kate Huihsuan Chen, Hsin-Ju Tai, Satoshi Ide, Timothy B Byrne, and Christopher W Johnson.
   Tidal modulation and tectonic implications of tremors in taiwan.
   Journal of Geophysical Research: Solid Earth, 123(7):5945–5964, 2018.
8. T Nishikawa, T Matsuzawa, K Ohta, N Uchida, T Nishimura, and S Ide.
   The slow earthquake spectrum in the japan trench illuminated by the s-net seafloor observatories.
   Science, 365(6455):808–813, 2019.
9. Demian M Saffer and Laura M Wallace.
   The frictional, hydrologic, metamorphic and thermal habitat of shallow slow earthquakes.
   Nature Geoscience, 8(8):594–600, 2015.
10. Gregory C Beroza and Satoshi Ide.
    Slow earthquakes and nonvolcanic tremor.
    Annual Review of Earth and Planetary Sciences, 39(1):271–296, 2011.
11. Noel M Bartlow, Shin'ichi Miyazaki, Andrew M Bradley, and Paul Segall.
    Space-time correlation of slip and tremor during the 2009 cascadia slow slip event.
    Geophysical Research Letters, 38(18), 2011.
12. Honn Kao, Kelin Wang, Herb Dragert, Jason Y Kao, and Garry Rogers.
    Estimating seismic moment magnitude (mw) of tremor bursts in northern cascadia: Implications for the "seismic efficiency" of episodic tremor and slip.
    Geophysical Research Letters, 37(19), 2010.
13. S R Chestler and K C Creager.
    Evidence for a scale-limited low-frequency earthquake source process.
    Journal of Geophysical Research: Solid Earth, 122(4):3099–3114, 2017.
14. Aaron G Wech and Noel M Bartlow.
    Slip rate and tremor genesis in cascadia.
    Geophysical Research Letters, 41(2):392–398, 2014.
15. William B Frank, Nikolaï M Shapiro, Allen L Husker, Vladimir Kostoglodov, Alexey Romanenko, and Michel Campillo.
    Using systematically characterized low-frequency earthquakes as a fault probe in guerrero, mexico.
    Journal of Geophysical Research: Solid Earth, 119(10):7686–7700, 2014.
16. Roland Bürgmann.
    The geophysics, geology and mechanics of slow fault slip.
    Earth and Planetary Science Letters, 495:112–134, 2018.
17. Joan Gomberg and the Cascadia 2007 and Beyond Working Group.
    Slow-slip phenomena in cascadia from 2007 and beyond: A review.
    Geological Society of America Bulletin, 122(7-8):963–978, 2010.
18. J C Hawthorne and N M Bartlow.
    Observing and modeling the spectrum of a slow slip event.
    Journal of Geophysical Research: Solid Earth, 123(5):4243–4265, 2018.

For Review Only

This manuscript has not yet undergone peer review

19. Geoffrey A Abers.
Seismic low-velocity layer at the top of subducting slabs: observations, predictions, and systematics.
Physics of the Earth and Planetary Interiors, 149(1-2):7–29, 2005.
20. David R Shelly, Gregory C Beroza, Satoshi Ide, and Sho Nakamula.
Low-frequency earthquakes in shikoku, japan, and their relationship to episodic tremor and slip.
Nature, 442(7099):188–191, July 2006.
21. Pascal Audet, Michael G Bostock, Nikolas I Christensen, and Simon M Peacock.
Seismic evidence for overpressured subducted oceanic crust and megathrust fault sealing.
Nature, 457(7225):76–78, January 2009.
22. Teh-Ru Alex Song, Donald V Helmberger, Michael R Brudzinski, Robert W Clayton, Paul Davis, Xyoli Pérez-Campos, and Shri K Singh.
Subducting slab ultra-slow velocity layer coincident with silent earthquakes in southern mexico.
Science, 324(5926):502–506, April 2009.
23. Aitaro Kato, Takashi Iidaka, Ryoya Ikuta, Yasuhiro Yoshida, Kei Katsumata, Takaya Iwasaki, Shin'ichi Sakai, Clifford Thurber, Noriko Tsumura, Koshun Yamaoka, Toshiki Watanabe, Takahiro Kunitomo, Fumihito Yamazaki, Makoto Okubo, Sadaomi Suzuki, and Naoshi Hirata.
Variations of fluid pressure within the subducting oceanic crust and slow earthquakes.
Geophysical Research Letters, 37(14), 2010.
24. Pascal Audet and Younghee Kim.
Teleseismic constraints on the geological environment of deep episodic slow earthquakes in subduction zone forearcs: A review.
Tectonophysics, 670:1–15, 2016.
25. Yoshihiro Hiramatsu, Tomoko Watanabe, and Kazushige Obara.
Deep low-frequency tremors as a proxy for slip monitoring at plate interface.
Geophysical Research Letters, 35(13), 2008.
26. Justin R Brown, Stephanie G Prejean, Gregory C Beroza, Joan S Gomberg, and Peter J Haeussler.
Deep low-frequency earthquakes in tectonic tremor along the alaska-aleutian subduction zone.
Journal of Geophysical Research: solid earth, 118(3):1079–1090, 2013.
27. Kathryn Materna, Noel Bartlow, Aaron Wech, Charles Williams, and Roland Bürgmann.
Dynamically triggered changes of plate interface coupling in southern cascadia.
Geophysical Research Letters, 46(22):12890–12899, 2019.
28. S M Peacock, N I Christensen, M G Bostock, and P Audet.
High pore pressures and porosity at 35 km depth in the cascadia subduction zone.
Geology, 39(5):471–474, 2011.
29. Xiang Gao and Kelin Wang.
Rheological separation of the megathrust seismogenic zone and episodic tremor and slip.
Nature, 543(7645):416–419, 2017.
30. Simon M Peacock and Roy D Hyndman.
Hydrous minerals in the mantle wedge and the maximum depth of subduction thrust earthquakes.
Geophysical Research Letters, 26(16):2517–2520, 1999.
31. Bradley R Hacker.
H2O subduction beyond arcs.
Geochemistry, Geophysics, Geosystems, 9(3), 2008.
32. Peter E van Keken, Bradley R Hacker, Ellen M Syracuse, and Geoff A Abers.
Subduction factory: 4. depth-dependent flux of H2O from subducting slabs worldwide.
Journal of Geophysical Research, 116(B1), 2011.
33. Pascal Audet and Andrew J Schaeffer.
Fluid pressure and shear zone development over the locked to slow slip region in cascadia.
Sci Adv, 4(3):eaar2982, March 2018.
34. Jonathan R Delph, Alan Levander, and Fenglin Niu.
Fluid controls on the heterogeneous seismic characteristics of the cascadia margin.

For Review Only

rspa.royalsocietypublishing.org Proc R Soc A 0000000

Geophysical Research Letters, 45(20), 2018.

35. Ikuo Katayama, Tatsuya Terada, Keishi Okazaki, and Wataru Tanikawa.
Episodic tremor and slow slip potentially linked to permeability contrasts at the moho.
Nature Geoscience, 5(10):731–734, 2012.
36. Seiya Kawano, Ikuo Katayama, and Keishi Okazaki.
Permeability anisotropy of serpentinite and fluid pathways in a subduction zone.
Geology, 39(10):939–942, 2011.
37. A C Ganzhorn, H Pilorgé, and B Reynard.
Porosity of metamorphic rocks and fluid migration within subduction interfaces.
Earth and Planetary Science Letters, 522:107–117, 2019.
38. Ralf T J Hansen, Michael G Bostock, and Nikolas I Christensen.
Nature of the low velocity zone in cascadia from receiver function waveform inversion.
Earth and Planetary Science Letters, 337-338:25–38, 2012.
39. G A Abers, L S MacKenzie, S Rondenay, Z Zhang, A G Wech, and K C Creager.
Imaging the source region of cascadia tremor and intermediate-depth earthquakes.
Geology, 37(12):1119–1122, 2009.
40. Andrew J Calvert, Leiph A Preston, and Amir M Farahbod.
Sedimentary underplating at the cascadia mantle-wedge corner revealed by seismic imaging.
Nature Geoscience, 4(8):545–548, 2011.
41. Philip E Wannamaker, Rob L Evans, Paul A Bedrosian, Martyn J Unsworth, Virginie Maris, and R Shane McGary.
Segmentation of plate coupling, fate of subduction fluids, and modes of arc magmatism in cascadia, inferred from magnetotelluric resistivity.
Geochemistry, Geophysics, Geosystems, 15(11):4230–4253, 2014.
42. N I Christensen.
Pore pressure and oceanic crustal seismic structure.
Geophysical Journal International, 79(2):411–423, 1984.
43. K Nishimura, S Uehara, and K Mizoguchi.
An alternative origin of high Vp/Vs anomalies in slow slip regions: Experimental constraints from the elastic wave velocity evolution of highly fractured rock.
Journal of Geophysical Research: Solid Earth, 124(5):5045–5059, 2019.
44. Roy D Hyndman and Simon M Peacock.
Serpentinization of the forearc mantle.
Earth and Planetary Science Letters, 212(3-4):417–432, 2003.
45. Junichi Nakajima and Akira Hasegawa.
Tremor activity inhibited by well-drained conditions above a megathrust.
Nat. Commun., 7:13863, December 2016.
46. Ray E Wells, Richard J Blakely, Aaron G Wech, Patricia A McCrory, and Andrew Michael.
Cascadia subduction tremor muted by crustal faults.
Geology, 45(6):515–518, 2017.
47. Pascal Audet and Roland Bürgmann.
Possible control of subduction zone slow-earthquake periodicity by silica enrichment.
Nature, 510(7505):389–392, June 2014.
48. K Ramachandran and R D Hyndman.
The fate of fluids released from subducting slab in northern cascadia.
Solid Earth, 3(1):121–129, 2012.
49. R D Hyndman, P A McCrory, A Wech, H Kao, and J Ague.
Cascadia subducting plate fluids channelled to fore-arc mantle corner: ETS and silica deposition.
Journal of Geophysical Research: Solid Earth, 120(6):4344–4358, 2015.
50. Yoshiyuki Tanaka, Aitaro Kato, Takayuki Sugano, Guangyu Fu, Xinlin Zhang, Masato Furuya, Wenke Sun, Shuhei Okubo, Shigeo Matsumoto, Masaki Honda, Yasuhiro Sugawara, Isao Ueda, Masaaki Kusaka, and Misao Ishihara.
Gravity changes observed between 2004 and 2009 near the tokai slow-slip area and prospects for detecting fluid flow during future slow-slip events.
Earth, Planets and Space, 62(12):905–913, 2010.
51. Yoshiyuki Tanaka, Takehito Suzuki, Yuichi Imanishi, Shuhei Okubo, Xinlin Zhang, Miwako Ando, Atsushi Watanabe, Mamoru Saka, Chiaki Kato, Shuichi Oomori, et al.

For Review Only

This manuscript has not yet undergone peer review

Temporal gravity anomalies observed in the tokai area and a possible relationship with slow slips.
Earth, Planets and Space, 70(1):25, 2018.

52. Jeremy M Gosselin, Pascal Audet, Clément Estève, Morgan McLellan, Stephen G Mosher, and Andrew J Schaeffer.
Seismic evidence for megathrust fault-valve behavior during episodic tremor and slip.
Sci Adv, 6(4):eaay5174, January 2020.
53. Junichi Nakajima and Naoki Uchida.
Repeated drainage from megathrusts during episodic slow slip.
Nature Geoscience, 11(5):351–356, 2018.
54. E Warren-Smith, B Fry, L Wallace, E Chon, S Henrys, A Sheehan, K Mochizuki, S Schwartz, S Webb, and S Lebedev.
Episodic stress and fluid pressure cycling in subducting oceanic crust during slow slip.
Nature Geoscience, 12(6):475–481, 2019.
55. Aaron G Wech and Kenneth C Creager.
A continuum of stress, strength and slip in the cascadia subduction zone.
Nature Geoscience, 4(9):624–628, 2011.
56. DA Schmidt and H Gao.
Source parameters and time-dependent slip distributions of slow slip events on the cascadia subduction zone from 1998 to 2008.
Journal of Geophysical Research: Solid Earth, 115(B4), 2010.
57. Takuya Nishimura, Takanori Matsuzawa, and Kazushige Obara.
Detection of short-term slow slip events along the nankai trough, southwest japan, using gnss data.
Journal of Geophysical Research: Solid Earth, 118(6):3112–3125, 2013.
58. Sylvain Michel, Adriano Gualandi, and Jean-Philippe Avouac.
Similar scaling laws for earthquakes and cascadia slow-slip events.
Nature, 574(7779):522–526, October 2019.
59. M Radiguet, F Cotton, M Vergnolle, M Campillo, A Walpersdorf, N Cotte, and V Kostoglodov.
Slow slip events and strain accumulation in the guerrero gap, mexico.
Journal of Geophysical Research: Solid Earth, 117(B4), 2012.
60. Baptiste Rousset, Roland Bürgmann, and Michel Campillo.
Slow slip events in the roots of the san andreas fault.
Sci Adv, 5(2):eaav3274, February 2019.
61. Shinzaburo Ozawa.
Long-term slow slip events along the nankai trough subduction zone after the 2011 tohoku earthquake in japan.
Earth, Planets and Space, 69(1), 2017.
62. Ryota Takagi, Naoki Uchida, and Kazushige Obara.
Along-Strike variation and migration of Long-Term slow slip events in the western nankai subduction zone, japan.
Journal of Geophysical Research: Solid Earth, 124(4):3853–3880, 2019.
63. Heidi Houston, Brent G Delbridge, Aaron G Wech, and Kenneth C Creager.
Rapid tremor reversals in cascadia generated by a weakened plate interface.
Nature Geoscience, 4(6):404–409, 2011.
64. William B Frank and Emily E Brodsky.
Daily measurement of slow slip from low-frequency earthquakes is consistent with ordinary earthquake scaling.
Sci Adv, 5(10):eaaw9386, October 2019.
65. Aaron G Wech, Kenneth C Creager, and Timothy I Melbourne.
Seismic and geodetic constraints on cascadia slow slip.
Journal of Geophysical Research: Solid Earth, 114(B10), 2009.
66. Kazushige Obara and Shutaro Sekine.
Characteristic activity and migration of episodic tremor and slow-slip events in central japan.
Earth, planets and space, 61(7):853–862, 2009.
67. Abhijit Ghosh, John E Vidale, Justin R Sweet, Kenneth C Creager, Aaron G Wech, Heidi Houston, and Emily E Brodsky.

For Review Only

rspa.royalsocietypublishing.org Proc R Soc A 0000000

Rapid, continuous streaking of tremor in cascadia.
Geochemistry, Geophysics, Geosystems, 11(12), 2010.

68. Yajun Peng, Allan M Rubin, Michael G Bostock, and John G Armbruster.
High-resolution imaging of rapid tremor migrations beneath southern vancouver island using cross-station cross correlations.
Journal of Geophysical Research: Solid Earth, 120(6):4317–4332, 2015.
69. Allan M Rubin and John G Armbruster.
Imaging slow slip fronts in cascadia with high precision cross-station tremor locations.
Geochemistry, Geophysics, Geosystems, 14(12):5371–5392, 2013.
70. Quentin Bletery and Jean-Mathieu Nocquet.
Slip bursts during coalescence of slow slip events in cascadia.
Nat. Commun., 11(1):2159, May 2020.
71. M G Bostock, A M Thomas, G Savard, L Chuang, and A M Rubin.
Magnitudes and moment-duration scaling of low-frequency earthquakes beneath southern vancouver island.
Journal of Geophysical Research: Solid Earth, 120(9):6329–6350, 2015.
72. SR Chestler and KC Creager.
A model for low-frequency earthquake slip.
Geochemistry, Geophysics, Geosystems, 18(12):4690–4708, 2017.
73. Amanda M Thomas, Gregory C Beroza, and David R Shelly.
Constraints on the source parameters of low-frequency earthquakes on the san andreas fault.
Geophysical Research Letters, 43(4):1464–1471, 2016.
74. A M Thomas, N M Beeler, Q Bletery, R Burgmann, and D R Shelly.
Using Low-Frequency earthquake families on the san andreas fault as deep creepmeters.
Journal of Geophysical Research: Solid Earth, 123(1):457–475, 2018.
75. William B Frank, Mathilde Radiguet, Baptiste Rousset, Nikolaï M Shapiro, Allen L Husker, Vladimir Kostoglodov, Nathalie Cotte, and Michel Campillo.
Uncovering the geodetic signature of silent slip through repeating earthquakes.
Geophysical Research Letters, 42(8):2774–2779, 2015.
76. John G Armbruster, Won-Young Kim, and Allan M Rubin.
Accurate tremor locations from coherent S and P waves.
Journal of Geophysical Research: Solid Earth, 119(6):5000–5013, 2014.
77. Kazushige Obara, Takanori Matsuzawa, Sachiko Tanaka, and Takuto Maeda.
Depth-dependent mode of tremor migration beneath kii peninsula, nankai subduction zone.
Geophysical Research Letters, 39(10), 2012.
78. Kazushige Obara, Sachiko Tanaka, Takuto Maeda, and Takanori Matsuzawa.
Depth-dependent activity of non-volcanic tremor in southwest japan.
Geophysical Research Letters, 37(13), 2010.
79. Koki Idehara, Suguru Yabe, and Satoshi Ide.
Regional and global variations in the temporal clustering of tectonic tremor activity.
Earth, Planets and Space, 66(1), 2014.
80. Satoshi Ide, Gregory C Beroza, David R Shelly, and Takahiko Uchide.
A scaling law for slow earthquakes.
Nature, 447(7140):76–79, May 2007.
81. Jessica C Hawthorne, Michael G Bostock, Alexandra A Royer, and Amanda M Thomas.
Variations in slow slip moment rate associated with rapid tremor reversals in cascadia.
Geochemistry, Geophysics, Geosystems, 17(12):4899–4919, 2016.
82. Quentin Bletery, Amanda M Thomas, Alan W Rempel, and Jeanne L Hardebeck.
Imaging shear strength along subduction faults.
Geophysical Research Letters, 44(22):11,329–11,339, 2017.
83. Quentin Bletery, Amanda M Thomas, Jessica C Hawthorne, Robert M Skarbek, Alan W Rempel, and Randy D Krogstad.
Characteristics of secondary slip fronts associated with slow earthquakes in cascadia.
Earth and Planetary Science Letters, 463:212–220, 2017.
84. Trevor W Thomas, John E Vidale, Heidi Houston, Kenneth C Creager, Justin R Sweet, and Abhijit Ghosh.
Evidence for tidal triggering of high-amplitude rapid tremor reversals and tremor streaks in northern cascadia.

For Review Only

Geophysical Research Letters, 40(16):4254–4259, 2013.

85. Heidi Houston.
Low friction and fault weakening revealed by rising sensitivity of tremor to tidal stress.
Nature Geoscience, 8(5):409–415, 2015.
86. Akio Katsumata and Noriko Kamaya.
Low-frequency continuous tremor around the moho discontinuity away from volcanoes in the southwest japan.
Geophysical Research Letters, 30(1):20–21, 2003.
87. David R Shelly, Gregory C Beroza, and Satoshi Ide.
Non-volcanic tremor and low-frequency earthquake swarms.
Nature, 446(7133):305–307, March 2007.
88. Masaru Nakano, Suguru Yabe, Hiroko Sugioka, Masanao Shinohara, and Satoshi Ide.
Event size distribution of shallow tectonic tremor in the nankai trough.
Geophysical Research Letters, 46(11):5828–5836, 2019.
89. M G Bostock, A M Thomas, A M Rubin, and N I Christensen.
On corner frequencies, attenuation, and low-frequency earthquakes.
Journal of Geophysical Research: Solid Earth, 122(1):543–557, 2017.
90. J Gomberg, K Creager, J Sweet, J Vidale, A Ghosh, and A Hotovec.
Earthquake spectra and near-source attenuation in the cascadia subduction zone.
J. Geophys. Res. [Solid Earth], 117(B5), 2012.
91. M G Bostock, A A Royer, E H Hearn, and S M Peacock.
Low frequency earthquakes below southern vancouver island.
Geochemistry, Geophysics, Geosystems, 13(11), 2012.
92. Satoshi Ide, David R Shelly, and Gregory C Beroza.
Mechanism of deep low frequency earthquakes: Further evidence that deep non-volcanic tremor is generated by shear slip on the plate interface.
Geophysical Research Letters, 34(3), 2007.
93. Yoshihiro Ito, Kazushige Obara, Katsuhiko Shiomi, Shutaro Sekine, and Hitoshi Hirose.
Slow earthquakes coincident with episodic tremors and slow slip events.
Science, 315(5811):503–506, January 2007.
94. Satoshi Ide and Suguru Yabe.
Universality of slow earthquakes in the very low frequency band.
Geophysical Research Letters, 41(8):2786–2793, 2014.
95. Alexandra A Hutchison.
Inter-episodic tremor and slip event episodes of quasi-spatiotemporally discrete tremor and very low frequency earthquakes in cascadia suggestive of a connective underlying, heterogeneous process.
Geophysical Research Letters, 47(3), 2020.
96. Satoshi Ide and Suguru Yabe.
Two-Dimensional probabilistic cell automaton model for broadband slow earthquakes.
Pure and Applied Geophysics, 176(3):1021–1036, 2019.
97. J Gomberg, A Wech, K Creager, K Obara, and D Agnew.
Reconsidering earthquake scaling.
Geophysical Research Letters, 43(12):6243–6251, 2016.
98. Justin L Rubinstein, Joan Gomberg, John E Vidale, Aaron G Wech, Honn Kao, Kenneth C Creager, and Garry Rogers.
Seismic wave triggering of nonvolcanic tremor, episodic tremor and slip, and earthquakes on vancouver island.
Journal of Geophysical Research, 114, 2009.
99. Kevin Chao and Kazushige Obara.
Triggered tectonic tremor in various types of fault systems of japan following the 2012mw8.6 sumatra earthquake.
Journal of Geophysical Research: Solid Earth, 121(1):170–187, 2016.
100. Jessica C Hawthorne and Allan M Rubin.
Tidal modulation of slow slip in cascadia.
Journal of Geophysical Research, 115(B9), 2010.
101. Justin L Rubinstein, Mario La Rocca, John E Vidale, Kenneth C Creager, and Aaron G Wech.
Tidal modulation of nonvolcanic tremor.

For Review Only

Science, 319(5860):186–189, January 2008.
102. A A Royer, A M Thomas, and M G Bostock.
Tidal modulation and triggering of low-frequency earthquakes in northern cascadia.
Journal of Geophysical Research: Solid Earth, 120(1):384–405, 2015.
103. N M Beeler, Amanda Thomas, Roland Bürgmann, and David Shelly.
Inferring fault rheology from low-frequency earthquakes on the san andreas.
Journal of Geophysical Research: Solid Earth, 118(11):5976–5990, 2013.
104. N M Beeler, Amanda Thomas, Roland Bürgmann, and David Shelly.
Constraints on friction, dilatancy, diffusivity, and effective stress from Low-Frequency earthquake rates on the deep san andreas fault.
Journal of Geophysical Research: Solid Earth, 123(1):583–605, 2018.
105. Sarah C Penniston-Dorland, Matthew J Kohn, and Craig E Manning.
The global range of subduction zone thermal structures from exhumed blueschists and eclogites: Rocks are hotter than models.
Earth and Planetary Science Letters, 428:243–254, 2015.
106. P Agard, A Plunder, S Angiboust, G Bonnet, and J Ruh.
The subduction plate interface: rock record and mechanical coupling (from long to short timescales).
Lithos, 320-321:537–566, 2018.
107. S Maruyama, J G Liou, and M Terabayashi.
Blueschists and eclogites of the world and their exhumation.
International Geology Review, 38(6):485–594, 1996.
108. W G Ernst.
Systematics of large-scale tectonics and age progressions in alpine and Circum-Pacific blueschist belts.
Tectonophysics, 26(3-4):229–246, 1975.
109. J R Carden, W Connelly, R B Forbes, and D L Turner.
Blueschists of the kodiak islands, alaska: An extension of the seldovia schist terrane.
Geology, 5(9):529, 1977.
110. J P Platt.
Dynamics of orogenic wedges and the uplift of high-pressure metamorphic rocks.
GSA Bulletin, 97(9):1037–1053, September 1986.
111. E H Brown and M C Blake.
Correlation of early cretaceous blueschists in washington, oregon and northern california.
Tectonics, 6(6):795–806, 1987.
112. W G Ernst.
Tectonic history of subduction zones inferred from retrograde blueschist P-T paths.
Geology, 16(12):1081, 1988.
113. John P Platt, Whitney M Behr, Katherine Johanesen, and Jason R Williams.
The Betic-Rif arc and its orogenic hinterland: A review.
Annual Review of Earth and Planetary Sciences, 41(1):313–357, 2013.
114. L Jolivet.
Subduction tectonics and exhumation of high-pressure metamorphic rocks in the mediterranean orogens.
American Journal of Science, 303(5):353–409, 2003.
115. Uwe Ring, Johannes Glodny, Thomas Will, and Stuart Thomson.
The hellenic subduction system: High-Pressure metamorphism, exhumation, normal faulting, and Large-Scale extension.
Annual Review of Earth and Planetary Sciences, 38(1):45–76, 2010.
116. K Bucher.
Blueschists, eclogites, and decompression assemblages of the Zermatt-Saas ophiolite: High-pressure metamorphism of subducted tethys lithosphere.
American Mineralogist, 90(5-6):821–835, 2005.
117. J G Liou, Xiaomin Wang, R G Coleman, Zh M Zhang, and S Maruyama.
Blueschists in major suture zones of china.
Tectonics, 8(3):609–619, 1989.
118. A I Okay.
Alpine-Himalayan blueschists.

For Review Only

This manuscript has not yet undergone peer review

Annual Review of Earth and Planetary Sciences, 17(1):55–87, 1989.

119. Jean-Pierre Brun and Claudio Faccenna.
Exhumation of high-pressure rocks driven by slab rollback.
Earth and Planetary Science Letters, 272(1-2):1–7, 2008.
120. Stéphane Guillot, Keiko Hattori, Philippe Agard, Stéphane Schwartz, and Olivier Vidal.
Exhumation processes in oceanic and continental subduction contexts: A review.
Subduction Zone Geodynamics, pages 175–205, 2009.
121. Ronald L Shreve and Mark Cloos.
Dynamics of sediment subduction, melange formation, and prism accretion.
Journal of Geophysical Research, 91(B10):10229, 1986.
122. Peter E van Keken, Ikuko Wada, Geoffrey A Abers, Bradley R Hacker, and Kelin Wang.
Mafic High-Pressure rocks are preferentially exhumed from warm subduction settings.
Geochemistry, Geophysics, Geosystems, 19(9):2934–2961, 2018.
123. Susan Ellis, Christopher Beaumont, and O Adrian Pfiffner.
Geodynamic models of crustal-scale episodic tectonic accretion and underplating in subduction zones.
Journal of Geophysical Research: Solid Earth, 104(B7):15169–15190, 1999.
124. David W Scholl, Roland von Huene, Tracy L Vallier, and David G Howell.
Sedimentary masses and concepts about tectonic processes at underthrust ocean margins.
Geology, 8(12):564, 1980.
125. Mark Cloos and Ronald L Shreve.
Subduction-channel model of prism accretion, melange formation, sediment subduction, and subduction erosion at convergent plate margins: 1. background and description.
Pure and Applied Geophysics PAGEOPH, 128(3-4):455–500, 1988.
126. Gianni Balestro, Gianfranco Fioraso, and Bruno Lombardo.
Geological map of the monviso massif (western alps).
Journal of Maps, 9(4):623–634, 2013.
127. Laura Federico, Laura Crispini, Marco Scambelluri, and Giovanni Capponi.
Ophiolite mélange zone records exhumation in a fossil subduction channel.
Geology, 35(6):499, 2007.
128. Peter D Clift.
A revised budget for cenozoic sedimentary carbon subduction.
Reviews of Geophysics, 55(1):97–125, 2017.
129. Mihai N Ducea and Alan D Chapman.
Sub-magmatic arc underplating by trench and forearc materials in shallow subduction systems; a geologic perspective and implications.
Earth-Science Reviews, 185:763–779, 2018.
130. Donna Eberhart-Phillips and Martin Reyners.
Plate interface properties in the northeast hikurangi subduction zone, new zealand, from converted seismic waves.
Geophysical Research Letters, 26(16):2565–2568, 1999.
131. J D Morris, W P Leeman, and F Tera.
The subducted component in island arc lavas: constraints from be isotopes and B–Be systematics.
Nature, 344(6261):31–36, 1990.
132. S A Peacock.
Fluid processes in subduction zones.
Science, 248(4953):329–337, April 1990.
133. Jay J Ague and Stefan Nicolescu.
Carbon dioxide released from subduction zones by fluid-mediated reactions.
Nature Geoscience, 7(5):355–360, 2014.
134. Christopher Beaumont, Susan Ellis, and Adrian Pfiffner.
Dynamics of sediment subduction-accretion at convergent margins: Short-term modes, long-term deformation, and tectonic implications.
Journal of Geophysical Research: Solid Earth, 104(B8):17573–17601, 1999.
135. Whitney M Behr and Thorsten W Becker.
Sediment control on subduction plate speeds.
Earth and Planetary Science Letters, 502:166–173, 2018.

For Review Only

rspa.royalsocietypublishing.org Proc R Soc A 0000000

136. Richard D Jarrard.
Subduction fluxes of water, carbon dioxide, chlorine, and potassium.
Geochemistry, Geophysics, Geosystems, 4(5), 2003.
137. T M Kusky, B F Windley, I Safonova, K Wakita, J Wakabayashi, A Polat, and M Santosh.
Recognition of ocean plate stratigraphy in accretionary orogens through earth history: A record of 3.8billion years of sea floor spreading, subduction, and accretion.
Gondwana Research, 24(2):501–547, 2013.
138. Jonas B Ruh, Laetitia Le Pourhiet, Ph Agard, Evguenii Burov, and Taras Gerya.
Tectonic slicing of subducting oceanic crust along plate interfaces: Numerical modeling.
Geochemistry, Geophysics, Geosystems, 16(10):3505–3531, 2015.
139. Walter Kurz, Franz Neubauer, and Edgar Dachs.
Eclogite meso- and microfabrics: implications for the burial and exhumation history of eclogites in the tauern window (eastern alps) from P-T-d paths.
Tectonophysics, 285(1-2):183–209, 1998.
140. Alissa J Kotowski and Whitney M Behr.
Length scales and types of heterogeneities along the deep subduction interface: Insights from exhumed rocks on syros island, greece.
Geosphere, 15(4):1038–1065, 2019.
141. Timothy J Rawling and Gordon S Lister.
Large-scale structure of the eclogite–blueschist belt of new caledonia.
Journal of Structural Geology, 24(8):1239–1258, 2002.
142. Peter B Davis and Donna L Whitney.
Petrogenesis and structural petrology of high-pressure metabasalt pods, sivrihisar, turkey.
Contributions to Mineralogy and Petrology, 156(2):217–241, 2008.
143. Whitney M Behr, Alissa J Kotowski, and Kyle T Ashley.
Dehydration-induced rheological heterogeneity and the deep tremor source in warm subduction zones.
Geology, 46(5):475–478, 2018.
144. Masami Okada, Naoki Uchida, and Shigeki Aoki.
Statistical forecasts and tests for small interplate repeating earthquakes along the japan trench.
Earth, Planets and Space, 64(8):703–715, 2012.
145. Michele Paulatto, Mireille Laigle, Audrey Galve, Philippe Charvis, Martine Sapin, Gaye Bayrakci, Mikael Evain, and Heidrun Kopp.
Dehydration of subducting slow-spread oceanic lithosphere in the lesser antilles.
Nat. Commun., 8:15980, July 2017.
146. Andrea Festa, Gianni Balestro, Yildirim Dilek, and Paola Tartarotti.
A jurassic oceanic core complex in the high-pressure monviso ophiolite (western alps, NW italy).
Lithosphere, page L458.1, 2015.
147. Gaku Kimura and John Ludden.
Peeling oceanic crust in subduction zones.
Geology, 23(3):217, 1995.
148. Peter Clift.
Controls on tectonic accretion versus erosion in subduction zones: Implications for the origin and recycling of the continental crust.
Reviews of Geophysics, 42(2), 2004.
149. Mark Cloos.
Lithospheric buoyancy and collisional orogenesis: Subduction of oceanic plateaus, continental margins, island arcs, spreading ridges, and seamounts.
Geological Society of America Bulletin, 105(6):715, 1993.
150. Charles R Stern.
Subduction erosion: Rates, mechanisms, and its role in arc magmatism and the evolution of the continental crust and mantle.
Gondwana Research, 20(2-3):284–308, 2011.
151. Roland von Huene, Roland von Huene, César R Ranero, and Paola Vannucchi.
Generic model of subduction erosion.
Geology, 32(10):913, 2004.

For Review Only

This manuscript has not yet undergone peer review

152. W M Behr and J P Platt.
Kinematic and thermal evolution during two-stage exhumation of a mediterranean subduction complex.
Tectonics, 31(4), 2012.

153. John Wakabayashi, EM Moores, D Sloan, and DL Stout.
Subduction and the rock record: Concepts developed in the franciscan complex, california.
Classic Cordilleran concepts: A view from California: Geological Society of America Special Paper, 338:123–133, 1999.

154. Mark A Helper.
Deformation and high P/T metamorphism in the central part of the condrey mountain window, north-central klamath mountains, california and oregon.
Geological Society of America Memoirs, pages 125–142, 1986.

155. A Takasu, S R Wallis, S Banno, and R D Dallmeyer.
Evolution of the sambagawa metamorphic belt, japan.
Lithos, 33(1-3):119–133, 1994.

156. Carl E Jacobson, Felix R Oyarzabal, and Gordon B Haxel.
Subduction and exhumation of the Pelona-Orocopia-Rand schists, southern california.
Geology, 24(6):547, 1996.

157. Valentin Laurent, Laurent Jolivet, Vincent Roche, Romain Augier, Stéphane Scaillet, and Giovanni Luca Cardello.
Strain localization in a fossilized subduction channel: Insights from the cycladic blueschist unit (syros, greece).
Tectonophysics, 672-673:150–169, 2016.

158. Sara Wassmann and Bernhard Stöckhert.
Rheology of the plate interface — dissolution precipitation creep in high pressure metamorphic rocks.
Tectonophysics, 608:1–29, 2013.

159. Whitney Maria Behr and John Paul Platt.
Rheological evolution of a mediterranean subduction complex.
Journal of Structural Geology, 54:136–155, 2013.

160. Daeyeong Kim, Ikuo Katayama, Katsuyoshi Michibayashi, and Tatsuki Tsujimori.
Deformation fabrics of natural blueschists and implications for seismic anisotropy in subducting oceanic crust.
Physics of the Earth and Planetary Interiors, 222:8–21, 2013.

161. Yi Cao, Haemyeong Jung, and Shuguang Song.
Microstructures and petro-fabrics of lawsonite blueschist in the north qilian suture zone, NW china: Implications for seismic anisotropy of subducting oceanic crust.
Tectonophysics, 628:140–157, 2014.

162. Daeyeong Kim, Ikuo Katayama, Katsuyoshi Michibayashi, and Tatsuki Tsujimori.
Rheological contrast between glaucophane and lawsonite in naturally deformed blueschist from diablo range, california.
Island Arc, 22(1):63–73, 2013.

163. Melodie E French and Cailey B Condit.
Slip partitioning along an idealized subduction plate boundary at deep slow slip conditions.
Earth and Planetary Science Letters, 528:115828, 2019.

164. John P Platt, Haoran Xia, and William Lamborn Schmidt.
Rheology and stress in subduction zones around the aseismic/seismic transition.
Progress in Earth and Planetary Science, 5(1), 2018.

165. Haoran Xia and John P Platt.
Structural and rheological evolution of the laramide subduction channel in southern california.
Solid Earth, 8(2):379–403, 2017.

166. Christopher J Tulley, Åke Fagereng, and Kohtaro Ujiie.
Hydrous oceanic crust hosts megathrust creep at low shear stresses.
Sci Adv, 6(22):eaba1529, May 2020.

167. Bernhard Stöckhert.
Stress and deformation in subduction zones: insight from the record of exhumed metamorphic rocks.

For Review Only

rspa.royalsocietypublishing.org Proc R Soc A 0000000

Geological Society, London, Special Publications, 200(1):255–274, 2002.

168. R H Sibson.
Transient discontinuities in ductile shear zones.
Journal of Structural Geology, 2(1-2):165–171, 1980.
169. Åke Fagereng and Richard H Sibson.
Mélange rheology and seismic style.
Geology, 38(8):751–754, 2010.
170. Peter B Kelemen and Greg Hirth.
A periodic shear-heating mechanism for intermediate-depth earthquakes in the mantle.
Nature, 446(7137):787–790, April 2007.
171. R J Knipe and R P Wintsch.
Heterogeneous deformation, foliation development, and metamorphic processes in a polyphase mylonite.
Metamorphic Reactions, pages 180–210, 1985.
172. Philip Wehrens, Alfons Berger, Max Peters, Thomas Spillmann, and Marco Herwegh.
Deformation at the frictional-viscous transition: Evidence for cycles of fluid-assisted embrittlement and ductile deformation in the granitoid crust.
Tectonophysics, 693:66–84, 2016.
173. Samuel Angiboust, Josephine Kirsch, Onno Oncken, Johannes Glodny, Patrick Monié, and Erik Rybacki.
Probing the transition between seismically coupled and decoupled segments along an ancient subduction interface.
Geochemistry, Geophysics, Geosystems, 16(6):1905–1922, 2015.
174. Christie D Rowe, Francesca Meneghini, and J Casey Moore.
Textural record of the seismic cycle: strain-rate variation in an ancient subduction thrust.
Geological Society, London, Special Publications, 359(1):77–95, 2011.
175. Darrel S Cowan.
Do faults preserve a record of seismic slip? a field geologist's opinion.
Journal of Structural Geology, 21(8-9):995–1001, 1999.
176. Christie D Rowe and W Ashley Griffith.
Do faults preserve a record of seismic slip: A second opinion.
Journal of Structural Geology, 78:1–26, 2015.
177. Hakon Austrheim and Torgeir B Andersen.
Pseudotachylytes from corsica: fossil earthquakes from a subduction complex.
Terra Nova, 16(4):193–197, 2004.
178. Raik Bachmann, Onno Oncken, Johannes Glodny, Wolfgang Seifert, Viktoria Georgieva, and Masafumi Sudo.
Exposed plate interface in the european alps reveals fabric styles and gradients related to an ancient seismogenic coupling zone.
Journal of Geophysical Research, 114(B5), 2009.
179. Christen D Rowe, J Casey Moore, Francesca Meneghini, and Alexander W McKeirnan.
Large-scale pseudotachylytes and fluidized cataclasites from an ancient subduction thrust fault.
Geology, 33(12):937, 2005.
180. Kohtaro Ujiie, Haruka Yamaguchi, Arito Sakaguchi, and Shoichi Toh.
Pseudotachylytes in an ancient accretionary complex and implications for melt lubrication during subduction zone earthquakes.
Journal of Structural Geology, 29(4):599–613, 2007.
181. Noah John Phillips, Christie D Rowe, and Kohtaro Ujiie.
For how long are pseudotachylytes strong? rapid alteration of basalt-hosted pseudotachylytes from a shallow subduction complex.
Earth and Planetary Science Letters, 518:108–115, 2019.
182. Darrel S Cowan.
Structural styles in mesozoic and cenozoic mélanges in the western cordillera of north america.
Geological Society of America Bulletin, 96(4):451, 1985.
183. Loren A Raymond.
Melanges: Their Nature, Origin, and Significance.

For Review Only

This manuscript has not yet undergone peer review

Geological Society of America, 1984.

184. Mark Cloos.
Flow melanges: Numerical modeling and geologic constraints on their origin in the franciscan subduction complex, california.
Geological Society of America Bulletin, 93(4):330, 1982.

185. Andrea Festa, Gian Andrea Pini, Yildirim Dilek, and Giulia Codegone.
Mélanges and mélange-forming processes: a historical overview and new concepts.
International Geology Review, 52(10-12):1040–1105, 2010.

186. Nicholas W Hayman and Luc L Lavier.
The geologic record of deep episodic tremor and slip.
Geology, 42(3):195–198, 2014.

187. Jacqueline E Reber, Nicholas W Hayman, and Luc L Lavier.
Stick-slip and creep behavior in lubricated granular material: Insights into the brittle-ductile transition.
Geophysical Research Letters, 41(10):3471–3477, 2014.

188. Luc L Lavier, Richard A Bennett, and Ravindra Duddu.
Creep events at the brittle ductile transition.
Geochemistry, Geophysics, Geosystems, 14(9):3334–3351, 2013.

189. Sam Webber, Susan Ellis, and Åke Fagereng.
"virtual shear box" experiments of stress and slip cycling within a subduction interface mélange.
Earth and Planetary Science Letters, 488:27–35, 2018.

190. Adam Beall, Åke Fagereng, and Susan Ellis.
Strength of strained Two-Phase mixtures: Application to rapid creep and stress amplification in subduction zone mélange.
Geophysical Research Letters, 46(1):169–178, 2019.

191. Åke Fagereng and Sabine A M den Hartog.
Subduction megathrust creep governed by pressure solution and frictional–viscous flow.
Nature Geoscience, 10(1):51–57, 2017.

192. Sabine A M den Hartog, Sabine A M den Hartog, and Christopher J Spiers.
A microphysical model for fault gouge friction applied to subduction megathrusts.
Journal of Geophysical Research: Solid Earth, 119(2):1510–1529, 2014.

193. K R McCLAY.
Pressure solution and coble creep in rocks and minerals: a review.
Journal of the Geological Society, 134(1):57–70, 1977.

194. Ichiko Shimizu.
Kinetics of pressure solution creep in quartz: theoretical considerations.
Tectonophysics, 245(3-4):121–134, 1995.

195. Jean-Pierre Gratier, Dag K Dysthe, and François Renard.
The role of pressure solution creep in the ductility of the earth's upper crust.
Advances in Geophysics, pages 47–179, 2013.

196. Åke Fagereng, Francesca Remitti, and Richard H Sibson.
Shear veins observed within anisotropic fabric at high angles to the maximum compressive stress.
Nature Geoscience, 3(7):482–485, 2010.

197. Kohtaro Ujiie, Hanae Saishu, Åke Fagereng, Naoki Nishiyama, Makoto Otsubo, Haruna Masuyama, and Hiroyuki Kagi.
An explanation of episodic tremor and slow slip constrained by Crack-Seal veins and viscous shear in subduction mélange.
Geophysical Research Letters, 45(11):5371–5379, 2018.

198. Pascal Philippot.
"crack seal" vein geometry in eclogitic rocks.
Geodinamica Acta, 1(3):171–181, 1987.

199. John G Ramsay.
The crack–seal mechanism of rock deformation.
Nature, 284(5752):135–139, 1980.

200. S Angiboust, P Agard, P Yamato, and H Raimbourg.
Eclogite breccias in a subducted ophiolite: A record of intermediate-depth earthquakes?

For Review Only

rspa.royalsocietypublishing.org Proc R Soc A 0000000

Geology, 40(8):707–710, 2012.

201. Pascal Philippot and Herman L M van Roermund.
Deformation processes in eclogitic rocks: evidence for the rheological delamination of the oceanic crust in deeper levels of subduction zones.
Journal of Structural Geology, 14(8-9):1059–1077, 1992.
202. Daniel R Viete, Bradley R Hacker, Mark B Allen, Gareth G E Seward, Mark J Tobin, Chris S Kelley, Gianfelice Cinque, and Andrew R Duckworth.
Metamorphic records of multiple seismic cycles during subduction.
Sci Adv, 4(3):eaaq0234, March 2018.
203. J D Rimstidt and H L Barnes.
The kinetics of silica-water reactions.
Geochimica et Cosmochimica Acta, 44(11):1683–1699, 1980.
204. D M Fisher, A J Smye, C Marone, P E Keken, and A Yamaguchi.
Kinetic models for healing of the subduction interface based on observations of ancient accretionary complexes.
Geochemistry, Geophysics, Geosystems, 2019.
205. Susan L Brantley, Brian Evans, Stephen H Hickman, and David A Crerar.
Healing of microcracks in quartz: Implications for fluid flow.
Geology, 18(2):136, 1990.
206. David L Smith and Brian Evans.
Diffusional crack healing in quartz.
Journal of Geophysical Research: Solid Earth, 89(B6):4125–4135, 1984.
207. Stephan Taetz, Timm John, Michael Bröcker, Carl Spandler, and Andreas Stracke.
Fast intraslab fluid-flow events linked to pulses of high pore fluid pressure at the subducted plate interface.
Earth and Planetary Science Letters, 482:33–43, 2018.
208. Simon M Peacock.
Thermal and metamorphic environment of subduction zone episodic tremor and slip.
Journal of Geophysical Research, 114, 2009.
209. Simon M Peacock.
The importance of blueschist → eclogite dehydration reactions in subducting oceanic crust.
Geological Society of America Bulletin, 105(5):684–694, 1993.
210. S A Miller, W van der Zee, D L Olgaard, and J A D Connolly.
A fluid-pressure feedback model of dehydration reactions: experiments, modelling, and application to subduction zones.
Tectonophysics, 370(1-4):241–251, 2003.
211. J A D Connolly.
The mechanics of metamorphic fluid expulsion.
Elements, 6(3):165–172, 2010.
212. Sarah Incel, Nadège Hilairet, Loïc Labrousse, Timm John, Damien Deldicque, Thomas Ferrand, Yanbin Wang, Jörg Renner, Luiz Morales, and Alexandre Schubnel.
Laboratory earthquakes triggered during eclogitization of lawsonite-bearing blueschist.
Earth and Planetary Science Letters, 459:320–331, 2017.
213. Oliver Plümper, Timm John, Yuri Y Podladchikov, Johannes C Vrijmoed, and Marco Scambelluri.
Fluid escape from subduction zones controlled by channel-forming reactive porosity.
Nature Geoscience, 10(2):150–156, 2017.
214. David P Dobson, Philip G Meredith, and Stephen A Boon.
Simulation of subduction zone seismicity by dehydration of serpentine.
Science, 298(5597):1407–1410, November 2002.
215. Keishi Okazaki and Greg Hirth.
Dehydration of lawsonite could directly trigger earthquakes in subducting oceanic crust.
Nature, 530(7588):81–84, February 2016.
216. Luigi Burlini, Giulio Di Toro, and Philip Meredith.
Seismic tremor in subduction zones: Rock physics evidence.
Geophysical Research Letters, 36(8), 2009.
217. Anne-Line Auzende, Javier Escartin, Nicolas P Walte, Stéphane Guillot, Greg Hirth, and Daniel J Frost.

For Review Only

This manuscript has not yet undergone peer review

Deformation mechanisms of antigorite serpentinite at subduction zone conditions determined from experimentally and naturally deformed rocks.
Earth and Planetary Science Letters, 411:229–240, 2015.

218. Melodie E French, Greg Hirth, and Keishi Okazaki.
Fracture-induced pore fluid pressure weakening and dehydration of serpentinite.
Tectonophysics, 767:228168, 2019.
219. J Perrillat, I Daniel, K Koga, B Reynard, H Cardon, and W Crichton.
Kinetics of antigorite dehydration: A real-time x-ray diffraction study.
Earth and Planetary Science Letters, 236(3-4):899–913, 2005.
220. Nadege Hilairet, Bruno Reynard, Yanbin Wang, Isabelle Daniel, Sebastien Merkel, Norimasa Nishiyama, and Sylvain Petitgirard.
High-pressure creep of serpentine, interseismic deformation, and initiation of subduction.
Science, 318(5858):1910–1913, December 2007.
221. Bradley R Hacker, Simon M Peacock, Geoffrey A Abers, and Stephen D Holloway.
Subduction factory 2. are intermediate-depth earthquakes in subducting slabs linked to metamorphic dehydration reactions?
Journal of Geophysical Research: Solid Earth, 108(B1), 2003.
222. Åke Fagereng and Johann F A Diener.
Non-volcanic tremor and discontinuous slab dehydration.
Geophysical Research Letters, 38(15), 2011.
223. Rob M Skarbek and Alan W Rempel.
Dehydration-induced porosity waves and episodic tremor and slip.
Geochemistry, Geophysics, Geosystems, 17(2):442–469, 2016.
224. Matthew S Tarling, Steven A F Smith, and James M Scott.
Fluid overpressure from chemical reactions in serpentinite within the source region of deep episodic tremor.
Nature Geoscience, 12(12):1034–1042, 2019.
225. Teruo Yamashita and Alexandre Schubnel.
Slow slip generated by dehydration reaction coupled with slip-induced dilatancy and thermal pressurization.
Journal of Seismology, 20(4):1217–1234, 2016.
226. M Philippon, F Gueydan, P Pitra, and J-P Brun.
Preservation of subduction-related prograde deformation in lawsonite pseudomorph-bearing rocks.
Journal of Metamorphic Geology, 31(5):571–583, 2013.
227. D Hunziker, J-P Burg, E Moulas, E Reusser, and J Omrani.
Formation and preservation of fresh lawsonite: Geothermobarometry of the north makran blueschists, southeast iran.
Journal of Metamorphic Geology, 35(8):871–895, 2017.
228. Jean-Michel Caron and Guy Péquignot.
The transition between blueschists and lawsonite-bearing eclogites based on observations from corsican metabasalts.
Lithos, 19(3-4):205–218, 1986.
229. Katherine F Fornash, Donna L Whitney, and Nicholas C A Seaton.
Lawsonite composition and zoning as an archive of metamorphic processes in subduction zones.
Geosphere, 15(1):24–46, 2019.
230. Donna L Whitney, Katherine F Fornash, Patricia Kang, Edward D Ghent, Laure Martin, Aral I Okay, and Alberto Vitale Brovarone.
Lawsonite composition and zoning as tracers of subduction processes: A global review.
Lithos, page 105636, 2020.
231. Clémentine Hamelin, John B Brady, John T Cheney, John C Schumacher, Lindsey M Able, and Arianne J Sperry.
Pseudomorphs after lawsonite from syros, greece.
Journal of Petrology, 59(12):2353–2384, 2018.
232. Rémi Magott, Olivier Fabbri, and Marc Fournier.
Seismically-induced serpentine dehydration as a possible mechanism of water release in subduction zones. insights from the alpine corsica pseudotachylyte-bearing monte maggiore ophiolitic unit.

For Review Only

rspa.royalsocietypublishing.org Proc R Soc A 0000000

Lithos, 362-363:105474, 2020.

233. J Hermann, O Müntener, and M Scambelluri.
The importance of serpentinite mylonites for subduction and exhumation of oceanic crust.
Tectonophysics, 327(3-4):225–238, 2000.
234. Anne-Line Auzende, Stéphane Guillot, Bertrand Devouard, and Alain Baronnet.
Serpentinites in an alpine convergent setting: Effects of metamorphic grade and deformation on microstructures.
European Journal of Mineralogy, 18(1):21–33, 2006.
235. E H Hoogerduijn Strating, E H Hoogerduijn Strating, and R L M Vissers.
Dehydration-induced fracturing of eclogite-facies peridotites: Implications for the mechanical behaviour of subducting oceanic lithosphere.
Tectonophysics, 200(1-3):187–198, 1991.
236. Cristiano Collettini, André Niemeijer, Cecilia Viti, and Chris Marone.
Fault zone fabric and fault weakness.
Nature, 462(7275):907–910, 2009.
237. Diane E Moore and Michael J Rymer.
Talc-bearing serpentinite and the creeping section of the san andreas fault.
Nature, 448(7155):795–797, August 2007.
238. Sabine A M den Hartog, Sabine A M den Hartog, Demian M Saffer, and Christopher J Spiers.
The roles of quartz and water in controlling unstable slip in phyllosilicate-rich megathrust fault gouges.
Earth, Planets and Space, 66(1), 2014.
239. Michele Locatelli, A Verlaguet, P Agard, L Federico, and S Angiboust.
Intermediate-depth brecciation along the subduction plate interface (monviso eclogite, w. alps).
Lithos, 320-321:378–402, 2018.
240. Solenn Hertgen, Philippe Yamato, Luiz F G Morales, and Samuel Angiboust.
Evidence for brittle deformation events at eclogite-facies P-T conditions (example of the mt. emilius klippe, western alps).
Tectonophysics, 706-707:1–13, 2017.
241. José Alberto Padrón-Navarta, Andréa Tommasi, Carlos J Garrido, and Vicente López Sánchez-Vizcaíno.
Plastic deformation and development of antigorite crystal preferred orientation in high-pressure serpentinites.
Earth and Planetary Science Letters, 349-350:75–86, 2012.
242. Gray E Bebout and Sarah C Penniston-Dorland.
Fluid and mass transfer at subduction interfaces—the field metamorphic record.
Lithos, 240-243:228–258, 2016.
243. Reiner Klemd.
Metasomatism during High-Pressure metamorphism: Eclogites and Blueschist-Facies rocks.
In Daniel E Harlov and Håkon Austrheim, editors, *Metasomatism and the Chemical Transformation of Rock: The Role of Fluids in Terrestrial and Extraterrestrial Processes*, pages 351–413. Springer Berlin Heidelberg, Berlin, Heidelberg, 2013.
244. John Farver and Richard Yund.
Silicon diffusion in a natural quartz aggregate: constraints on solution-transfer diffusion creep.
Tectonophysics, 325(3-4):193–205, 2000.
245. Richard H Sibson.
Structural permeability of fluid-driven fault-fracture meshes.
Journal of Structural Geology, 18(8):1031–1042, 1996.
246. Christopher M Breeding, Jay J Ague, Michael Bröcker, and Edward W Bolton.
Blueschist preservation in a retrograded, high-pressure, low-temperature metamorphic terrane, tinos, greece: Implications for fluid flow paths in subduction zones.
Geochemistry, Geophysics, Geosystems, 4(1), 2003.
247. Gray E Bebout and Mark D Barton.
Fluid flow and metasomatism in a subduction zone hydrothermal system: Catalina schist terrane, california.
Geology, 17(11):976, 1989.

For Review Only

248. Jesús Muñoz-Montecinos, Samuel Angiboust, Aitor Cambeses, and Antonio García-Casco.
Multiple veining in a paleo–accretionary wedge: The metamorphic rock record of prograde dehydration and transient high pore-fluid pressures along the subduction interface (western series, central chile).
Geosphere, 16(3):765–786, 2020.
249. Stephan Taetz, Timm John, Michael Bröcker, and Carl Spandler.
Fluid–rock interaction and evolution of a high-pressure/low-temperature vein system in eclogite from new caledonia: insights into intraslab fluid flow processes.
Contributions to Mineralogy and Petrology, 171(11), 2016.
250. Jay J Ague.
Models of permeability contrasts in subduction zone mélange: Implications for gradients in fluid fluxes, syros and tinos islands, greece.
Chemical Geology, 239(3-4):217–227, 2007.
251. Gray E Bebout and Mark D Barton.
Tectonic and metasomatic mixing in a high-t, subduction-zone mélange—insights into the geochemical evolution of the slab–mantle interface.
Chemical Geology, 187(1-2):79–106, 2002.
252. Samuel Angiboust, Thomas Pettke, Jan C M De Hoog, Benoit Caron, and Onno Oncken.
Channelized fluid flow and eclogite-facies metasomatism along the subduction shear zone.
Journal of Petrology, 55(5):883–916, 2014.
253. Pascal Philippot and Jane Selverstone.
Trace-element-rich brines in eclogitic veins: implications for fluid composition and transport during subduction.
Contributions to Mineralogy and Petrology, 106(4):417–430, 1991.
254. Nathan C Collins, Gray E Bebout, Samuel Angiboust, Philippe Agard, Marco Scambelluri, Laura Crispini, and Timm John.
Subduction zone metamorphic pathway for deep carbon cycling: II. evidence from HP/UHP metabasaltic rocks and ophicarbonates.
Chemical Geology, 412:132–150, 2015.
255. A C Barnicoat and I Cartwright.
Focused fluid flow during subduction: Oxygen isotope data from high-pressure ophiolites of the western alps.
Earth and Planetary Science Letters, 132(1-4):53–61, 1995.
256. S R Getty and J Selverstone.
Stable isotopic and trace element evidence for restricted fluid migration in 2 GPa eclogites.
Journal of Metamorphic Geology, 12(6):747–760, 1994.
257. Thomas Zack and Timm John.
Channelization and reactive fluid flow in subducting slabs.
Geochimica et Cosmochimica Acta, 70(18):A728, 2006.
258. T Widmer.
Local origin of high pressure vein material in eclogite facies rocks of the Zermatt-Saas-Zone, switzerland.
American Journal of Science, 301(7):627–656, 2001.
259. Carl Spandler and Jörg Hermann.
High-pressure veins in eclogite from new caledonia and their significance for fluid migration in subduction zones.
Lithos, 89(1-2):135–153, 2006.
260. Timm John, Reiner Kle, Jun Gao, and Carl-Dieter Garbe-Schönberg.
Trace-element mobilization in slabs due to non steady-state fluid–rock interaction: Constraints from an eclogite-facies transport vein in blueschist (tianshan, china).
Lithos, 103(1-2):1–24, 2008.
261. Carl Spandler, Thomas Pettke, and Daniela Rubatto.
Internal and external fluid sources for eclogite-facies veins in the monviso meta-ophiolite, western alps: Implications for fluid flow in subduction zones.
Journal of Petrology, 52(6):1207–1236, 2011.
262. Jun Gao, Timm John, Reiner Kle, and Xianming Xiong.
Mobilization of Ti–Nb–Ta during subduction: Evidence from rutile-bearing dehydration segregations and veins hosted in eclogite, tianshan, NW china.

For Review Only

rspa.royalsocietypublishing.org Proc R Soc A 0000000

Geochimica et Cosmochimica Acta, 71(20):4974–4996, 2007.

263. Estibalitz Ukar and Mark Cloos.
Cataclastic deformation and metasomatism in the subduction zone of mafic blocks-in-mélange, san simeon, california.
Lithos, 346-347:105116, 2019.
264. Manfred Schliestedt and Alan Matthews.
Transformation of blueschist to greenschist facies rocks as a consequence of fluid infiltration, sifnos (cyclades), greece.
Contributions to Mineralogy and Petrology, 97(2):237–250, 1987.
265. Sarah C Penniston-Dorland, Julia K Gorman, Gray E Bebout, Philip M Piccoli, and Richard J Walker.
Reaction rind formation in the catalina schist: Deciphering a history of mechanical mixing and metasomatic alteration.
Chemical Geology, 384:47–61, 2014.
266. Bruce K Nelson.
Fluid flow in subduction zones: evidence from nd- and sr-isotope variations in metabasalts of the franciscan complex, california.
Contributions to Mineralogy and Petrology, 119(2-3):247–262, 1995.
267. G E Bebout.
Field-based evidence for devolatilization in subduction zones: implications for arc magmatism.
Science, 251(4992):413–416, January 1991.
268. Keishi Okazaki, Ikuo Katayama, and Hiroyuki Noda.
Shear-induced permeability anisotropy of simulated serpentinite gouge produced by triaxial deformation experiments.
Geophysical Research Letters, 40(7):1290–1294, 2013.
269. Naoki Nishiyama, Hirochika Sumino, and Kohtaro Ujiie.
Fluid overpressure in subduction plate boundary caused by mantle-derived fluids.
Earth and Planetary Science Letters, 538:116199, 2020.

For Review Only

This manuscript has not yet undergone peer review

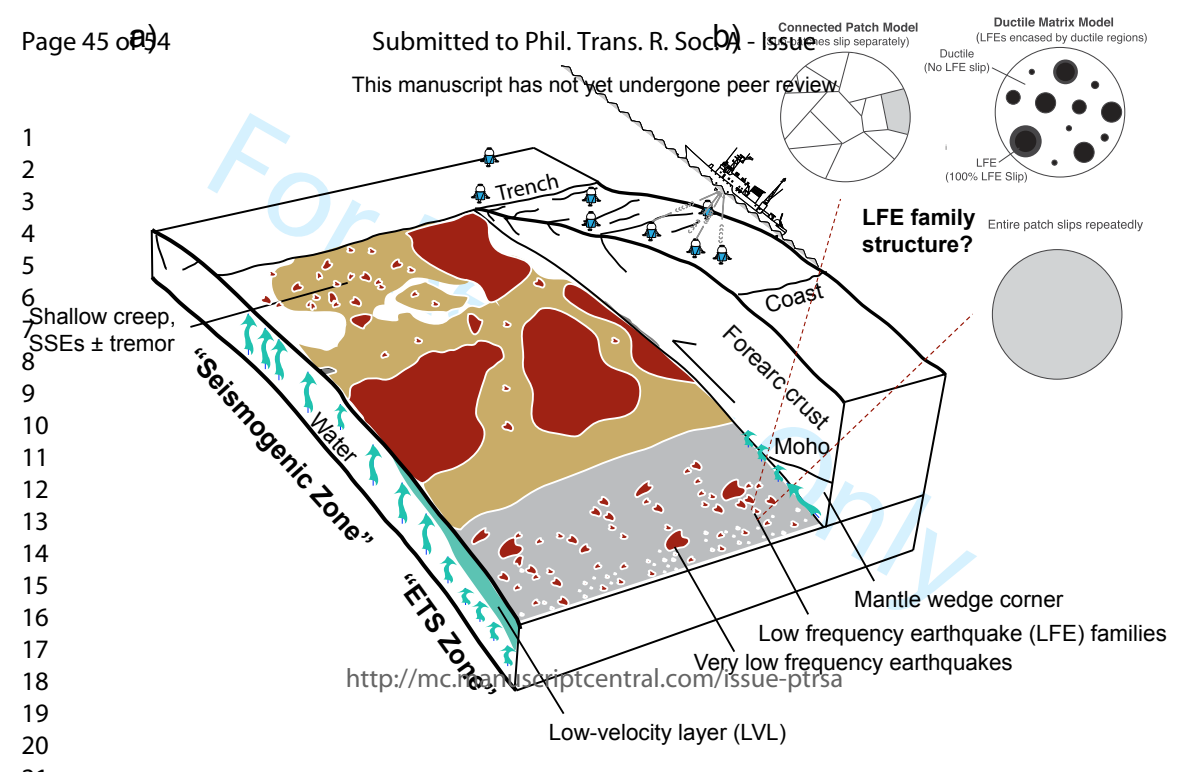

For Review Only

http://mc.manuscriptcentral.com/issue-ptrsa

This manuscript has not yet undergone peer review

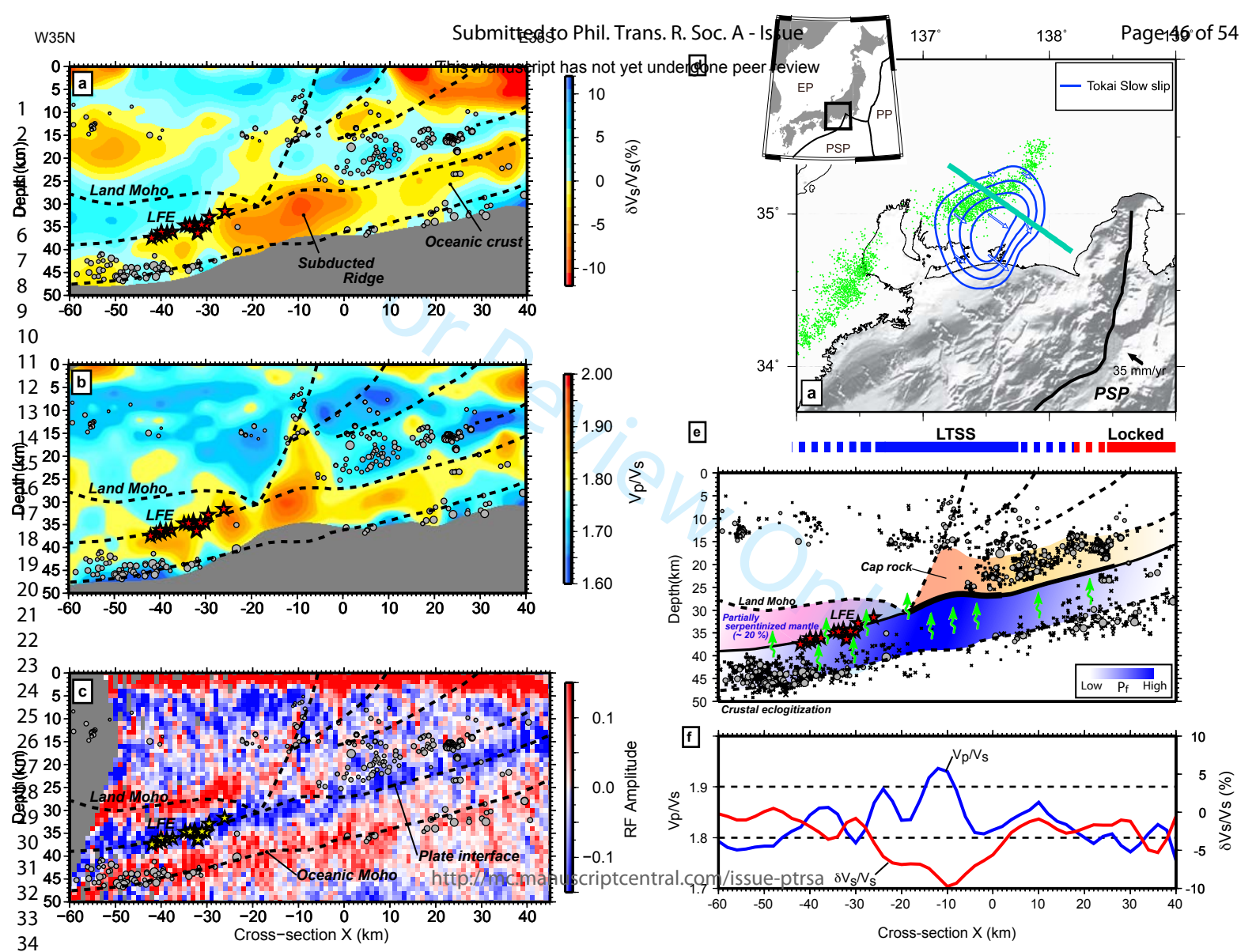

For Review Only
http://mc.manuscriptcentral.com/issue-ptrsa

Submitted to Phil. Trans. R. Soc. A - Issue
This manuscript has not yet undergone peer review

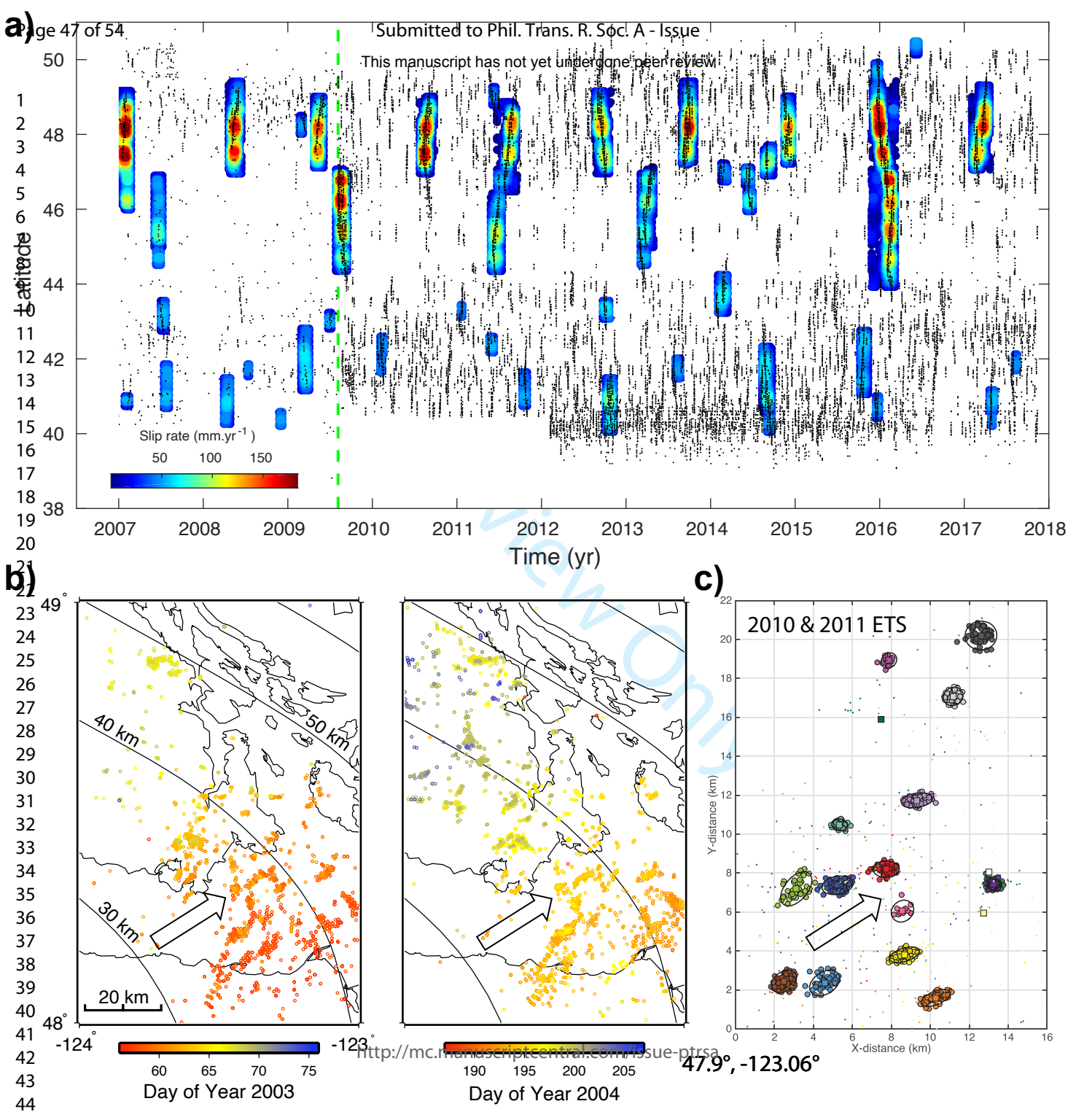

http://mc.manuscriptcentral.com/issue-ptrsa

This manuscript has not yet undergone peer review

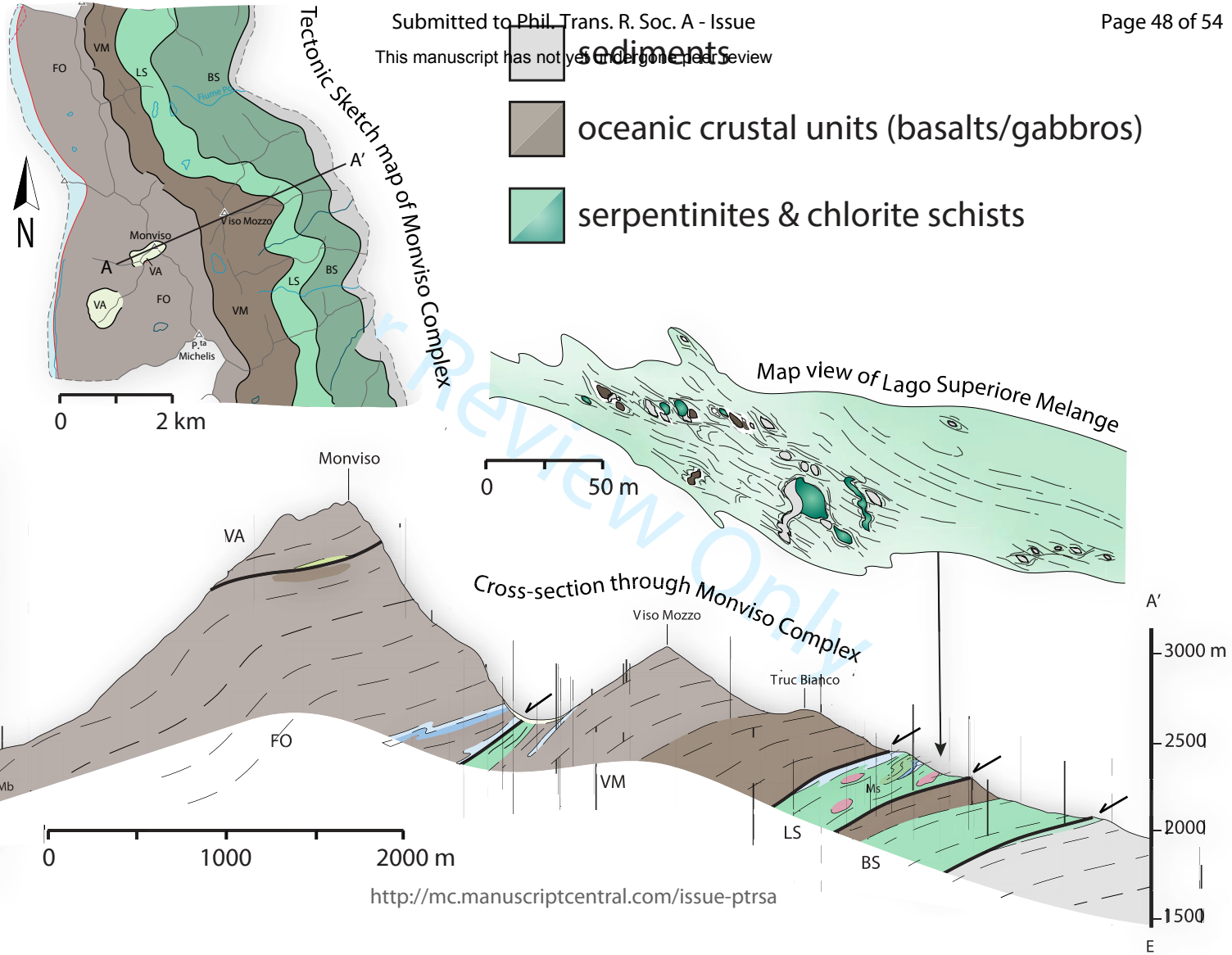

For Review Only

Submitted to Phil. Trans. R. Soc. A - Issue
This manuscript has not yet undergone peer review

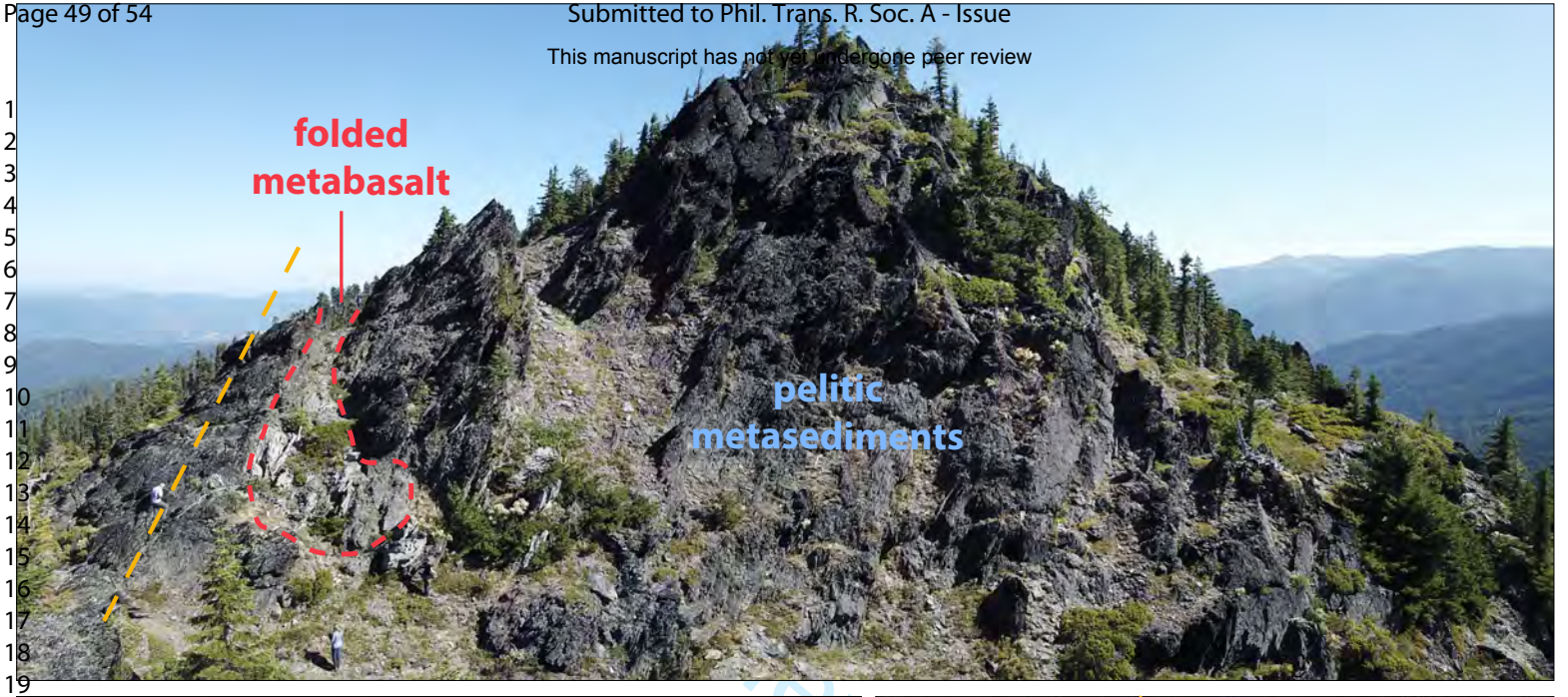

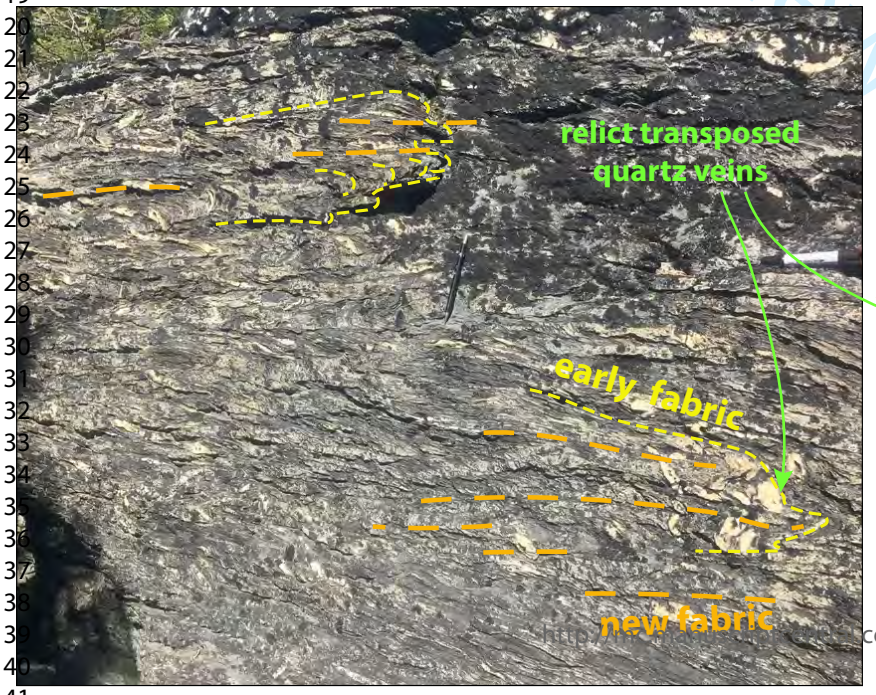

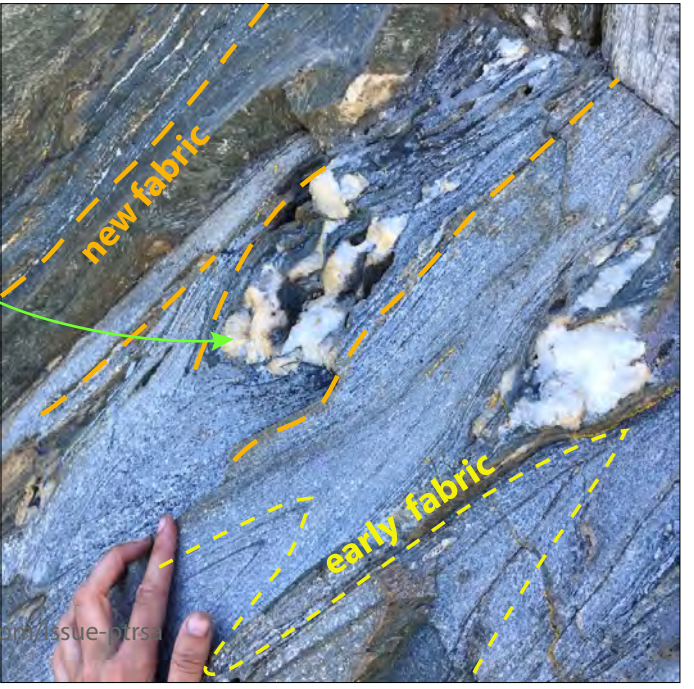

http://mc.manuscriptcentral.com/issue-ptrsa

This manuscript has not yet undergone peer review

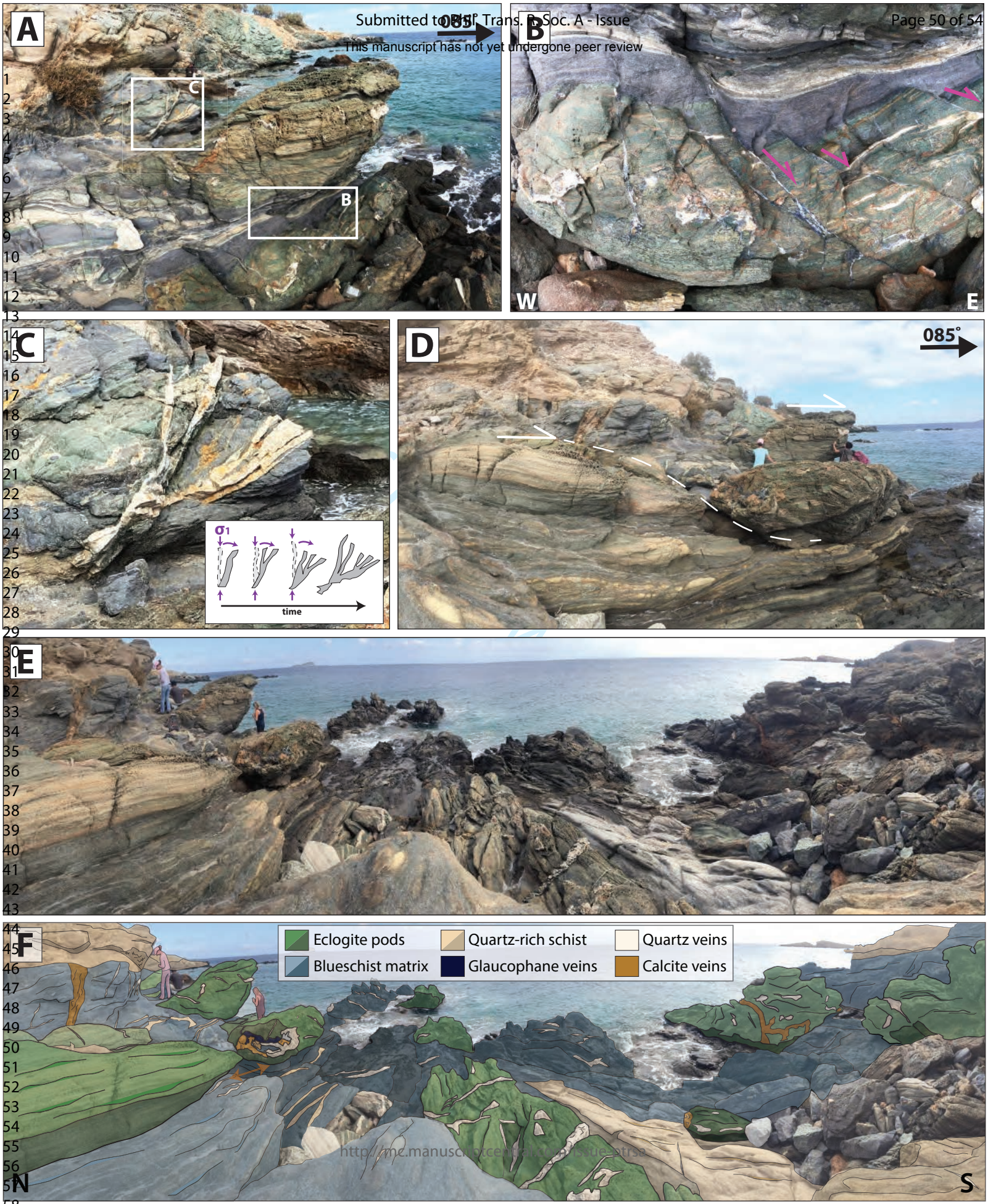

This manuscript has not yet undergone peer review

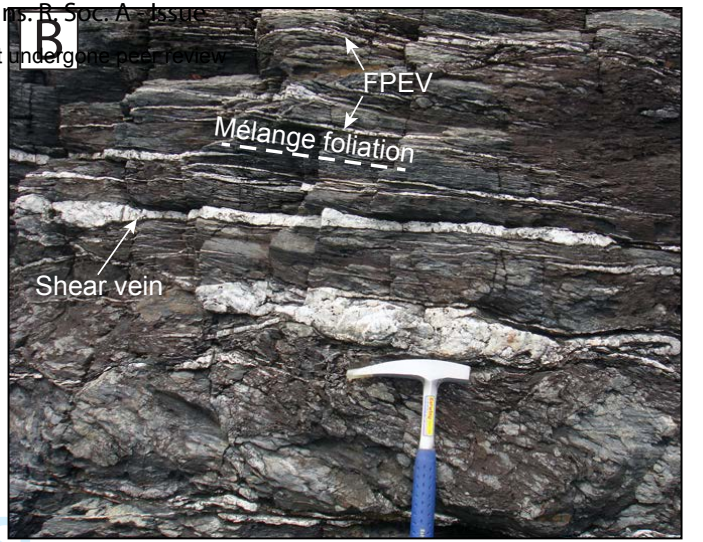

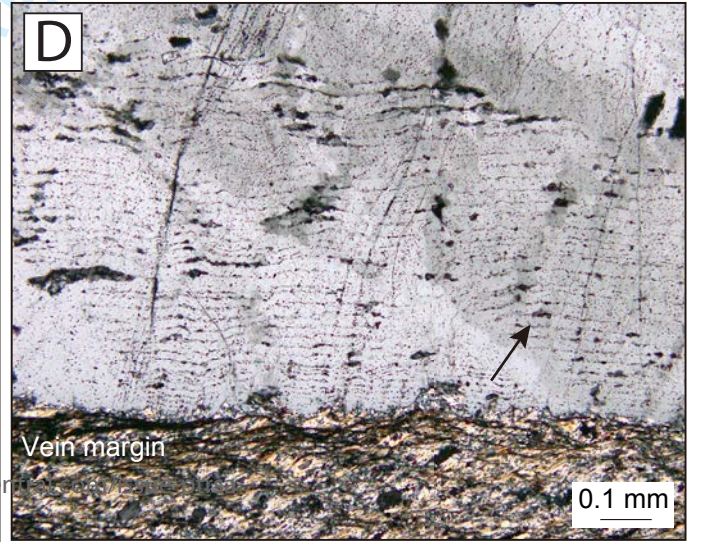

This manuscript has not yet undergone peer review

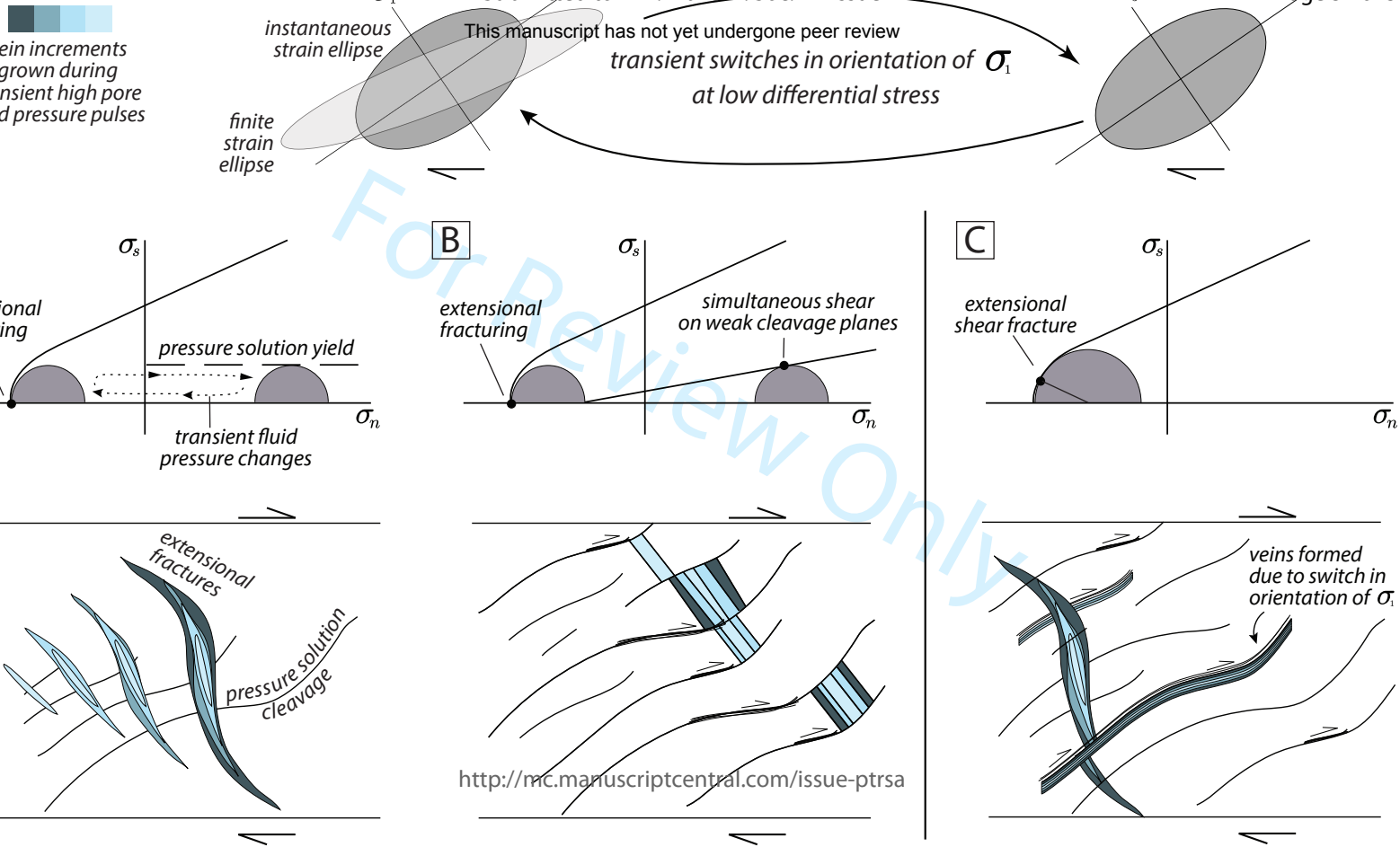

For Review Only

http://mc.manuscriptcentral.com/issue-ptrsa

Submitted to Phil. Trans. R. Soc. A - Issue
This manuscript has not yet undergone peer review

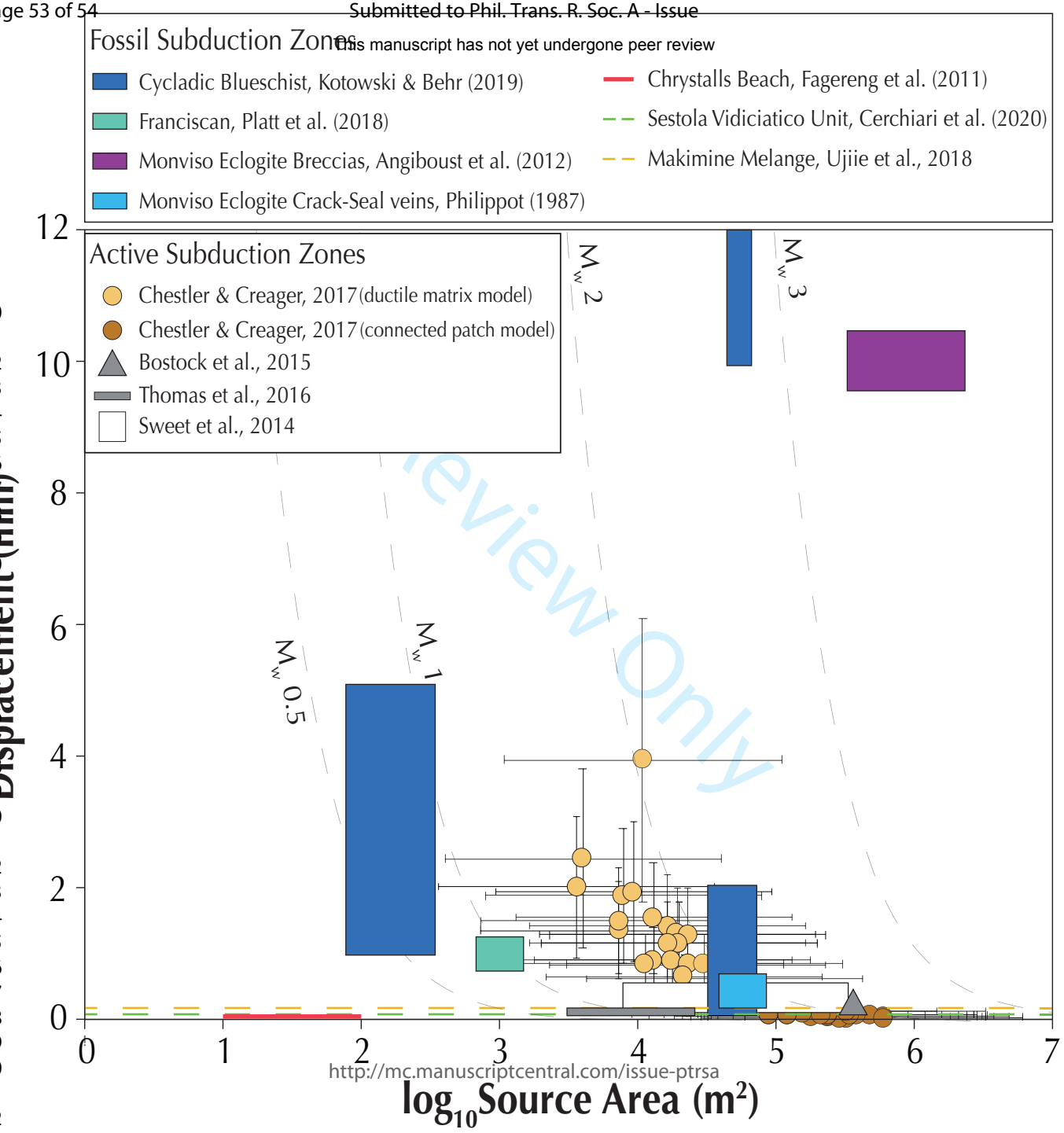

For Review Only

This manuscript has not yet undergone peer review

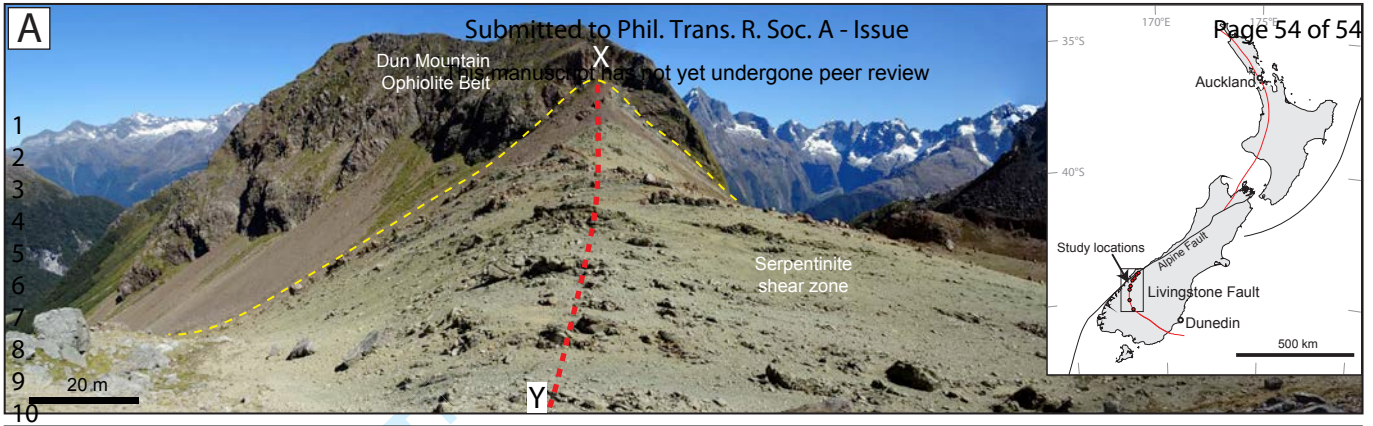

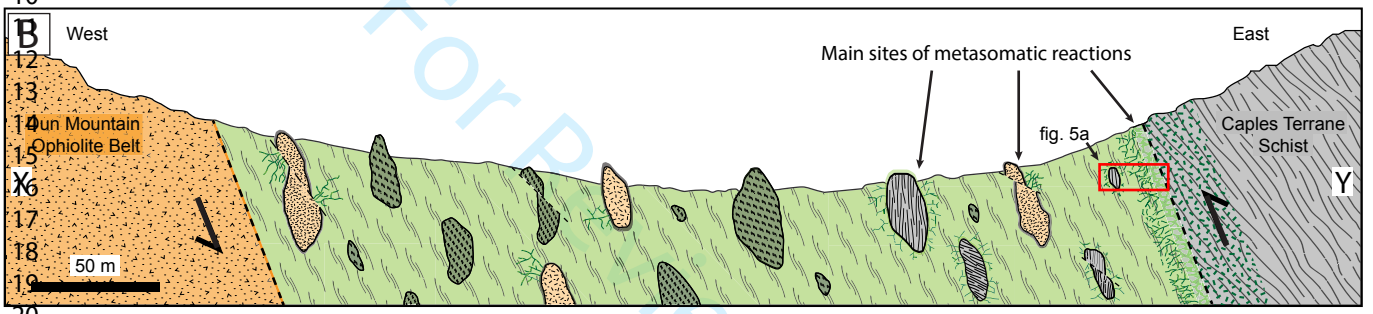

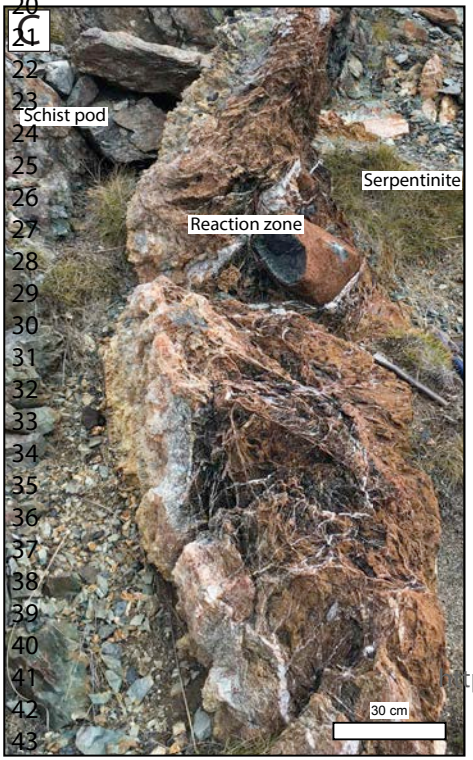

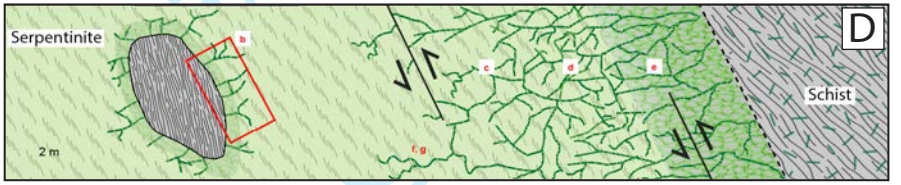

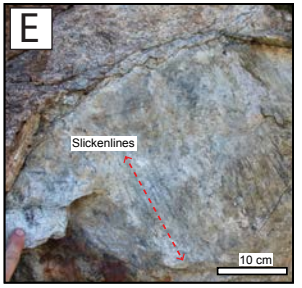

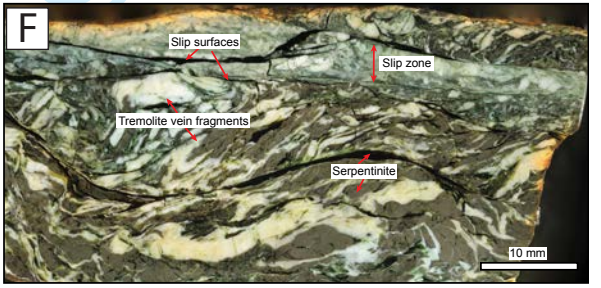

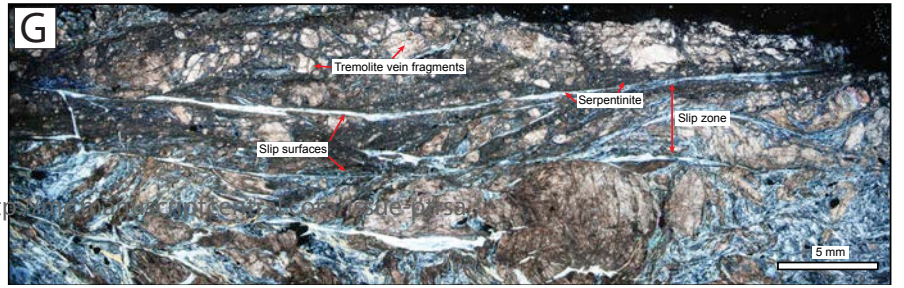

For Peer Review
http://mc.manuscriptcentral.com/rsta-phil-trans

Submitted to Phil. Trans. R. Soc. A - Issue
this manuscript has not yet undergone peer review